Doubly stochastic Poisson point process driven by fractal shot noise

Steven B. Lowen and Malvin C. Teich
Columbia Radiation Laboratory, Department of Electrical Engineering, Columbia University, New York, New York, 10027
(Received 18 October 1990)

We explore the behavior of the fractal-shot-noise-driven doubly stochastic Poisson point process (FSNDP), for which the associated impulse response functions assume a decaying power-law form. For a variety of parameters of the process, we obtain expressions for the count-number distribution and moments, Fano factor, normalized coincidence rate, power spectral density, and time probability densities. A number of these measures exhibit power-law dependencies, indicating fractal behavior. For certain parameters the power spectral density exhibits $1/f$-type behavior over a substantial range of frequencies, so that the process serves as a $1/f^{\alpha}$ point process for α in the range $0<\alpha<2$. We consider two physical processes that are well described by the FSNDP: Cherenkov radiation from a random stream of charged particles, and diffusion of randomly injected concentration packets.

I. INTRODUCTION

Stochastic point processes are useful for describing phenomena that occur at random points in time or space. Examples include the emission or absorption of photons or electrons, the arrival of customers at a queue and their subsequent departures from it, the detection of nuclear particles, the production of neural impulses in the nervous systems of living organisms, the occurrence of earthquakes, and the registration of vehicles passing through intersections. A point process is a complete mathematical description of these occurrence times. In general, the randomness is exhibited in varying times between events, varying numbers of events in a prespecified time, and more complex statistics such as how the events cluster together.

The most familiar stochastic point process is perhaps the one-dimensional homogeneous Poisson point process (HPP).[1] The HPP is characterized by a single, constant quantity, its rate, which is the number of events expected to occur in a unit interval. It plays the role that the Gaussian process does for continuous stochastic processes. Indeed, sums of independent point processes approach the homogeneous Poisson process under certain weak conditions, just as sums of independent continuous processes tend to a Gaussian limit in most cases. A fundamental property of the HPP is that it is memoryless; knowledge of the entire history and future of a given realization of a HPP yields no information about the behavior of the process at the present.

Other point processes do not share this memoryless property and therefore cannot be described in terms of a constant rate. An important example of an nonhomogeneous point process is the doubly stochastic Poisson point process (DSPP).[2] For this point process, the rate itself varies stochastically. Thus the DSPP displays two forms of randomness: that associated with the stochastically varying rate and that associated with the underlying Poisson nature of the process even if its rate were constant. The DSPP is useful for modeling phenomena ranging from photodetection[3] to sensory information processing.[4,5] A more detailed treatment of the history and properties of the DSPP is provided in Ref. 6 and the references therein.

One particular DSPP model which is appealing for its tractability, and yet lends itself to sophisticated analysis, is the shot-noise-driven doubly stochastic Poisson point process (SNDP).[6,7] In this special case, the rate of the Poisson process is determined by shot noise, which is itself a filtered version of another, homogeneous Poisson point process. Figure 1 schematically illustrates the SNDP as a two-stage stochastic process. The first stage is a HPP with constant rate μ. Its output becomes the input to a linear filter, which then produces shot noise at its output. This shot-noise process becomes the time-varying rate for the last stage, a second Poisson point process. The resulting point process is not homogeneous, but rather exhibits the variations of the shot-noise driving process. Thus the two forms of randomness inherent in the DSPP are explicitly separated into two Poisson processes in the SNDP, linked by a linear filter. The SNDP has been studied extensively and has applications ranging from ecology (in a two-dimensional version)[8] to photon and electron detection in a number of physical processes.[6]

In this paper we explore the properties of the fractal-shot-noise driven doubly stochastic Poisson point process, denoted fractal SNDP, FSNDP, or FSND-DSPP. In this case the linear filter used to generate the shot noise which drives the final Poison point process is described by a decaying power-law impulse response function, which imparts unique and useful properties to the resulting point process.

We examine various statistics of the FSNDP, including the time probability densities, number moments and distributions, Fano factor, normalized coincidence rate, and the power spectral density. Many of these statistics exhibit power-law dependencies on the counting or delay times over a significant range of times, indicating fractal behavior. We have identified several processes in which power-law behavior of the kind predicted by the FSNDP

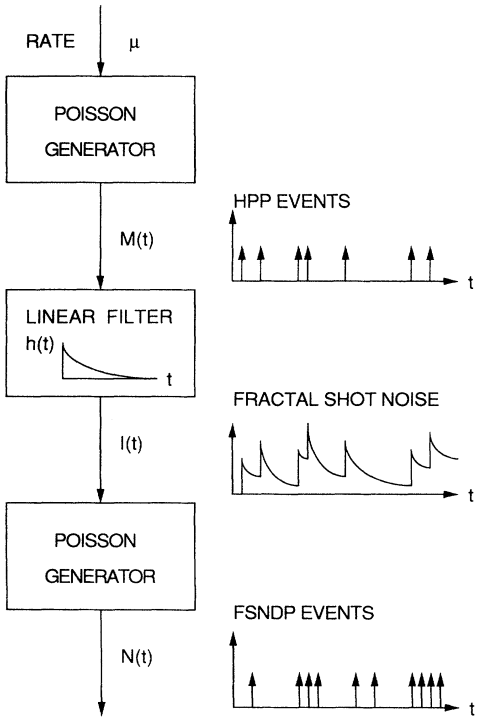

FIG. 1. A primary homogeneous Poisson point process $M(t)$ with constant rate μ serves as the input to a linear filter with impulse response function $h(t)$. The continuous-time stochastic process $I(t)$ at the output of this filter is shot noise, which serves as the random rate for another Poisson point process, whose output is $N(t)$. $N(t)$ is a special doubly stochastic Poisson point process (DSPP), known as a shot-noise-driven Poisson point process (SNDP). If $h(t)$ decays in power-law fashion, then $I(t)$ is fractal shot noise and $N(t)$ is a FSNDP.

is observed. We discuss two such processes: Cherenkov radiation, which arises from a random stream of high-velocity charged particles as they pass through a medium, and diffusion of randomly injected concentration packets across a distance. The FSNDP provides one promising model for describing the sequence of action potentials in primary fibers of the auditory nerve in mammals.[9]

II. CASCADE AND STOCHASTIC RATE FORMULATIONS

A DSPP may be defined in terms of a Poisson point process with stochastic rate as illustrated in Fig. 1. Alternatively, it can be described in terms of a two-stage cascade model in which a primary point process is viewed as directly generating a stochastic number of events in a secondary point process. The DSPP is a special case of a cluster point processes, the complete specification of which requires knowledge of three quantities: the primary event times at which each cluster begins, the probability distribution of the number of secondary events in each cluster, and a description of the times of occurrence of events within a cluster. In the Bartlett-Lewis cluster process,[10,11] primary events result from a HPP and the times between successive events in a given cluster are independent, identically distributed positive random variables. Thus the cluster resulting from a single primary event is a segment of a renewal process. In some other types of cluster point processes, the times between each secondary event and the *primary* event which produced it are specified. If these times are independent, identically distributed positive random variables, and the primary events are again described by a HPP, the result is a Neyman-Scott cluster process.[12,13] In general, for both types of cluster processes, the secondary events associated with different clusters are interleaved. Finally, any number of stages may be cascaded, yielding tertiary, quaternary, and higher-order processes.[14,15]

The SNDP may be formulated as a cluster process of the Neyman-Scott type, as defined above, or as a Poisson process with a stochastically varying shot-noise rate. The two formulations are isomorphic, as shown in Appendix A.

The stochastic rate formulation of the SNDP $N(t)$ is displayed schematically in Fig. 1. A primary homogeneous Poisson process $M(t)$ generates events $dM(t)$ at a mean rate μ. These events then pass through a linear filter with impulse response function $h(t)$. The output of this filter, denoted by $I(t)$, is shot noise, which serves as the input to the secondary Poisson process, which generates events $dN(t)$ at a time-varying rate equal to $I(t)$. Thus the SNDP is completely characterized by the primary-process rate μ and the impulse response function $h(t)$. For the FSNDP in particular, the impulse response function of the linear filter takes the form of a decaying power-law function. The fractal shot noise itself may also be completely characterized by its driving rate μ and associated impulse response function $h(t)$; the characteristics of the FSNDP point process therefore stem directly from those of fractal shot noise,[16–18] which we now proceed to examine.

III. FRACTAL SHOT NOISE

A. Power-law impulse response functions

A fractal-shot-noise process $I(t)$ may be expressed as an infinite sum of impulse response functions,

$$I(t) \equiv \sum_{j=-\infty}^{\infty} h(K_j, t - t_j) , \tag{1}$$

where the times t_j are random events $dM(t)$ from a homogeneous Poisson process $M(t)$ of rate μ, as shown in Fig. 1.[16–18] We define the impulse response function $h(\ ,\ )$ to be

$$h(K,t) \equiv \begin{cases} Kt^{-\beta}, & A < t < B \\ 0, & \text{otherwise} . \end{cases} \tag{2}$$

A sketch of a particular power-law impulse response function is provided in Fig. 2(a). The quantities $\{K_j\}$ in Eq. (1) represent a random sequence of amplitudes that are identically distributed and independent of each other

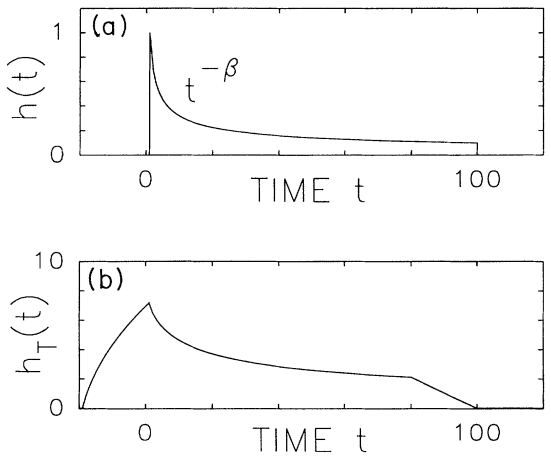

FIG. 2. (a) Linear plot of a particular power-law impulse response function $h(t)$ vs time t. (b) Linear plot of the associated integrated impulse response function $h_T(t)$ vs time t. ($\beta=\frac{1}{2}$, $A=1$, $B=100$, $K_0=1$, $T=20$.)

and of the Poisson process. In some cases we will require that K be deterministic (all K_j are fixed and equal to each other), and we indicate this with the zero subscript (K_0). Otherwise, K is a random variable. The impulse response function $h(\,,\,)$ is itself deterministic, and the parameters A, B, and β are deterministic and fixed. For all β, the range of the function may extend down to $A=0$ or up to $B=\infty$, and β may range between 0 and ∞ exclusive. It is useful to define several auxiliary parameters. For $\beta<1$ we define $\alpha\equiv 2(1-\beta)$, and for $\beta>1$ we define $D\equiv 1/\beta$. In general, we define a to be the mean area of the impulse response function

$$a\equiv\left\langle\int_0^\infty h(K,t)dt\right\rangle=\langle K\rangle\int_A^B t^{-\beta}dt\ , \tag{3}$$

where the angular brackets $\langle\ \rangle$ without any subscript represent expectation taken over the distribution of K. The mean and variance of the shot-noise process $I(t)$ are given by Campbell's theorem.[19,20] All properties are valid after $I(t)$ has reached steady state—that is, for finite t.

For most impulse response functions it is also useful to define a characteristic time, denoted τ_p. Heuristically, τ_p represents the time scale at which change in the value of an impulse response function takes place. One convenient definition of characteristic time depends on averaged quantities of the impulse response function and is given by

$$\tau_p\equiv\left\langle\int_0^\infty h(t)dt\right\rangle^2\Big/\left\langle\int_0^\infty h^2(t)dt\right\rangle\ . \tag{4}$$

For an exponential impulse response function, $h(t)=K_0\exp(-t/\tau)$, we obtain $\tau_p=2\tau$, while for a rectangular impulse response function Eq. (4) returns the width of the impulse response function itself. For $0<A\ll B<\infty$, the characteristic time of the power-law impulse response function as defined in Eq. (4) will depend on B for $\beta\le 1$ and on A for $\beta\ge\frac{1}{2}$. For a true fractal process, however, we require that $A=0$, $B=\infty$, or both; in that case, one or both of the integrals in Eq. (4) will not exist, depending on β. Rather than defining τ_p to be either zero or infinite, τ_p is left undefined if either of the two integrals in Eq. (4) is undefined. No useful definitions for τ_p have been found which will work for power-law impulse response functions with $A=0$ and $B=\infty$. Indeed, the notion of characteristic time has limited applicability for a fractal process, which by definition exhibits change on many time scales.

B. Fractal shot noise

Two results from fractal shot noise are of particular interest. First, for impulse response functions with $A=0$, $B=\infty$, and $\beta>1$, the resulting shot-noise process has an amplitude probability distribution that takes the form of a Lévy-stable random variable[21] of extreme asymmetry and dimension $D=1/\beta$ with $0<D<1$, for all rates μ of the Poisson driving process.[17,18] The associated moment generating function[22] is

$$Q_I(s)\equiv\langle\exp(-sI)\rangle_I=\exp[-\mu\langle K^D\rangle\Gamma(1-D)s^D]\ , \tag{5}$$

where the subscripted angle brackets $\langle\ \rangle_x$ represent expectation taken over the distribution of the subscripted variable or process x. For $B<\infty$ the amplitude probability distribution approaches this Lévy-stable random variable in the limit $\mu\to\infty$.[17,18] This result is surprising because the amplitude probability distribution does not converge to Gaussian form in the limit $\mu\to\infty$ and because it is not degenerate even though the impulse response function has infinite area a.

Second, for $B<\infty$ and $\beta<1$, the resulting power spectral density $S_I(f)$ varies as $1/f^\alpha$ for a substantial range of frequencies f, where $\alpha=2(1-\beta)$ lies in the range $0<\alpha<2$, and thus the process serves as a source of generalized $1/f$ noise.[16,18]

C. Integrated fractal shot noise

The time average of the shot-noise process $I(t)$ forms another random process that is important in the study of the FSNDP. Indeed, all of the first-order statistics of the FSNDP, including the time and number distributions, may be obtained from the first-order moment generating function of the integrated shot-noise process $W(t)$.[6] Noting that the time integral (time average) of a shot-noise process is another shot-noise process, we define

$$W(t)\equiv\int_t^{t+T}I(u)du\ , \tag{6}$$

with a corresponding impulse response function,

$$h_T(K,t)\equiv\int_t^{t+T}h(K,u)du\ . \tag{7}$$

A representative integrated impulse response function is sketched in Fig. 2(b).

The first-order moment generating function of the integrated shot-noise process $W(t)$ is given by[6]

$$
\begin{aligned}
Q_W(s) &\equiv \langle \exp(-sW) \rangle_W \\
&= \exp\left[\mu\left\langle \int_{-\infty}^{\infty} \{\exp[-sh_T(K,u)]-1\}du \right\rangle\right] \\
&= \exp\left\{\mu\left\langle \int_{-\infty}^{\infty} \left[\exp\left[-s\int_u^{u+T} h(K,t)dt\right]-1\right]du \right\rangle\right\} \\
&= \exp\left\{\mu\left\langle \int_{A-T}^{B} \left[\exp\left[-sK\int_{\max(u,A)}^{\min(u+T,B)} t^{-\beta}dt\right]-1\right]du \right\rangle\right\} \\
&= \exp\left\{\left\langle \int_{\mu A-\mu T}^{\mu B} \left[\exp\left[-sK\mu^{\beta-1}\int_{\max(y,\mu A)}^{\min(y+\mu T,\mu B)} x^{-\beta}dx\right]-1\right]dy \right\rangle\right\} ,
\end{aligned} \tag{8}
$$

where x and y are dimensionless variables defined by $x=\mu t$ and $y=\mu u$, respectively. In general, Eq. (8) cannot be evaluated in closed form, although simplifications are available for deterministic K_0 in some special cases. We consider first the case $\beta=1$. Here the moment generating function has the form

$$
\begin{aligned}
Q_W(s) = \exp\Bigg[& \mu\int_A^{A+T}[(A/u)^{sK_0}-1]du \\
& +\mu\int_{A+T}^{B}[(1-T/u)^{sK_0}-1]du \\
& +\mu\int_{B-T}^{B}[(u/B)^{sK_0}-1]du \Bigg] .
\end{aligned} \tag{9}
$$

In the special case $\beta=2$, $A=0$, and $B=\infty$, on the other hand, a closed-form expression emerges. It is

$$
Q_W(s) = \begin{cases} 1, & s=0 \\ \exp\left\{-\dfrac{\mu T}{2}-\mu s K_0\left[\exp\left[\dfrac{2sK_0}{T}\right]\right] \right. & \\ \left. \quad \times\left[\mathcal{K}_0\left[\dfrac{2sK_0}{T}\right]+\mathcal{K}_1\left[\dfrac{2sK_0}{T}\right]\right]\right\}, & s\neq 0 , \end{cases} \tag{10}
$$

where $\mathcal{K}_0(\,)$ and $\mathcal{K}_1(\,)$ are the modified Bessel functions of the second kind of order zero and unity, respectively. A detailed derivation of this expression is given in Appendix B.

IV. STATISTICAL PROPERTIES OF THE FRACTAL SNDP

The moment generating function $Q_n(s)$ for the number of events occurring in a counting time T may be derived from the moment generating function of the integrated rate $Q_W(s)$. The number of events is just the Poisson transform of the integrated rate,[23] so that

$$
Q_n(s) \equiv \langle \exp(-sn) \rangle_n = Q_W(1-e^{-s}) \tag{11}
$$

(see Appendix A). The first-order time statistics may in turn be determined from the first-order number statistics if they are known for all time T.

A. Infinite-area impulse response functions

The moment generating function $Q_W(s)$ in Eq. (10) is discontinuous at $s=0$. In fact, $Q_W(s)$ will be discontinuous at $s=0$ for $A=0$, $\beta\geq 1$, arbitrary B, and arbitrary K, either stochastic or deterministic. Since the impulse response function $h(t)$ then has infinite area in the infinitesimal interval after $t=0$, any time integral containing that interval will be infinite. The integrated shot-noise process $W(t)$ is obtained from $I(t)$ by integrating over a moving window of fixed length T, so it will be infinite for a period T after each primary event $dM(t)$. Since these primary events arise from a Poisson point process with average rate μ, the probability that no such events have occurred in an interval of length T is $\exp(-\mu T)$, resulting in

$$
\lim_{s\to 0} Q_W(s) = \Pr\{W<\infty\} = \exp(-\mu T) . \tag{12}
$$

Thus the integrated-rate amplitude W has a semidegenerate amplitude probability density function. However, in the limit $T\to 0$, the integration which produces $W(t)$ from $I(t)$ may be approximated by a simple multiplication by T, yielding $W(t)\approx TI(t)$, so that

$$
Q_W(s) \approx \exp[-\mu T^D \langle K^D \rangle \Gamma(1-D) s^D] , \tag{13}
$$

while for the number of counts n,

$$
Q_n(s) \approx \exp[-\mu T^D \langle K^D \rangle \Gamma(1-D)(1-e^{-s})^D] . \tag{14}
$$

For $\beta\leq 1$, with $A\to 0$ and $B\to\infty$, it is tempting to construct a limiting process since many interesting properties of the FSNDP occur within the time scale $A \ll T \ll B$. In this case, however, the resulting process $N(t)$ is trivial, since the shot-noise processes $I(t)$ and $W(t)$ are degenerate. For $B=\infty$ and $\beta\leq 1$, the shot-noise process $I(t)$ is infinite with probability one,[16,18] and therefore the integrated shot-noise process $W(t)$ will also be infinite and will have the completely degenerate moment generating function

$$
Q_W(s) = \begin{cases} 1, & s=0 \\ 0, & s\neq 0 . \end{cases} \tag{15}
$$

This result holds in general for any impulse response function with infinite area in its tail, as shown in Appendix C.

This problem may be circumvented by decreasing the height of the impulse response function, keeping the area in the tail finite. For example, if $\beta<1$, $A=0$, and K is proportional to $B^{\beta-1}$, then the area of the impulse response function will be fixed and finite even if B is increased without bound. However, in this case, the shot-noise process $I(t)$ will approach a constant value in the limit $B\rightarrow\infty$, as shown in Appendix D. In either case, the amplitude distribution of $I(t)$ will be trivial. Therefore, its time average $W(t)$ will also be trivial, and so will the resulting FSNDP, $N(t)$. In the first case, with infinite area in the tail of the impulse response function, $N(t)$ will be degenerate; with probability one there will be an infinite number of events occurring in any finite interval, and zero time between adjacent events. For the renormalized process, $W(t)=W$, a constant, and $N(t)$ will be a simple HPP with deterministic rate μa.

B. Counting statistics

The counting statistics describe the number of events n observed in a particular point process in a specified fixed time interval T. This reduces the point process to a discrete random number which may then be described in terms of its probability distribution, moments, or other statistical parameters.

1. Count probability distribution

The probability distribution of the count random variable n for any SNDP is given by the recurrence relation[6]

$$p(m+1)\equiv\Pr\{n=m+1\}=\frac{1}{m+1}\sum_{i=0}^{m}c_i p(m-i)\ , \tag{16}$$

where the coefficients c_i are defined by

$$c_i\equiv\frac{\mu}{i!}\left\langle\int_{-\infty}^{\infty}[h_T(K,t)]^{i+1}\exp[-h_T(K,t)]dt\right\rangle \tag{17}$$

and

$$p(0)=Q_W(1)$$
$$=\exp\left[\mu\left\langle\int_{-\infty}^{\infty}\{\exp[-h_T(K,t)]-1\}dt\right\rangle\right]\ . \tag{18}$$

Explicit formulas for $p(0)$ and c_i for the FSNDP are provided in Appendix E. These have been used to compute representative count probability distributions for the FSNDP for $\beta=\frac{1}{2}$, 1, and 2 for various counting times T, which are shown in Figs. 3, 4, and 5, respectively. For all plots, the mean number of counts $\langle n\rangle_n$ in the specified interval T is set to 10, and the impulse response function begins at $A=1$, ends at $B=10^5$, and has a deterministic K_0 such that the area $a=10$.

As indicated in Refs. 6 and 24, for any SNDP, if both the impulse response function area and mean number of counts are fixed while the counting time T is decreased, then the counting distribution will approach a Poisson distribution with the same mean as $T/\tau_p\rightarrow 0$. For long counting times ($T/\tau_p\gg 1$), the distribution approaches the Neyman type-A distribution[25] with the same mean. This distribution has a variance equal to $(1+a)$ times the mean, where a is the area of the impulse response function.[6] Each plot includes the Poisson distribution with a mean of 10, and the Neyman type-A distribution with a mean of 10 and a variance of 110 for comparison. The SNDP count probability distribution therefore interpolates between the Poisson and Neyman type-A distributions. Indeed, the two-parameter Neyman type-A distribution has been explicitly shown to serve as an excellent approximation for the counting statistics of the SNDP when the impulse response function $h(t)$ is exponential or rectangular.[26]

As the counting time is decreased, the rate of the primary Poisson process μ must increase to keep the total mean number of counts constant, since

$$\langle n\rangle_n=\mu a T\ . \tag{19}$$

For impulse response functions with

$$\left\langle\int_0^{\infty}h^2(K,t)dt\right\rangle<\infty \tag{20}$$

and $a<\infty$, the distributions of both the shot-noise amplitude probability density I and the integrated rate W will approach Gaussian forms, as provided by the central limit theorem.

For large counting times ($T/\tau_p\gg 1$) and for deterministic K_0, however, the integrated impulse response function is approximately rectangular:

$$h_T(K_0,t)\approx\begin{cases}\int_0^{\infty}h(K_0,t)dt=a, & -T<t\le 0\\ 0, & \text{otherwise}\ ,\end{cases} \tag{21}$$

so the integrated rate W will be Poisson distributed, taking on values equal to integer multiples of the area a.[27] The count probability distribution will then be the Poisson transform of the Poisson distributed rate W, resulting in the Neyman type-A distribution.[6]

For the FSNDP, holding the counting time T, the mean number of counts $\langle n\rangle_n$, and the impulse response function area a all fixed, but varying the power-law exponent β, yields a family of counting distributions spanning the range between the Poisson and the Neyman type-A distributions. This results from the nature of power-law impulse response functions. For $\beta<1$, most of the area a of the impulse response function is in the tail, with correspondingly little of the area near the onset. Thus this impulse response function exhibits less variation over its duration compared to an impulse response function with $\beta>1$, and the resulting shot-noise process will have correspondingly less variance, leading to a Poisson-like distribution, all other parameters remaining unchanged. For impulse response functions with $\beta>1$, the amplitude characteristics will exhibit more variation, leading to a larger variance and therefore the counting distribution will approach the Neyman type-A form. This relation may also be expressed in terms of the characteristic time of the impulse response function, τ_p. A small power-law exponent β will lead to a large τ_p. Therefore, if the counting time T is held fixed as β decreases, the counting distribution will tend to the short counting time limit, leading to a Poisson distribution. Conversely, for large β, the characteristic time will be

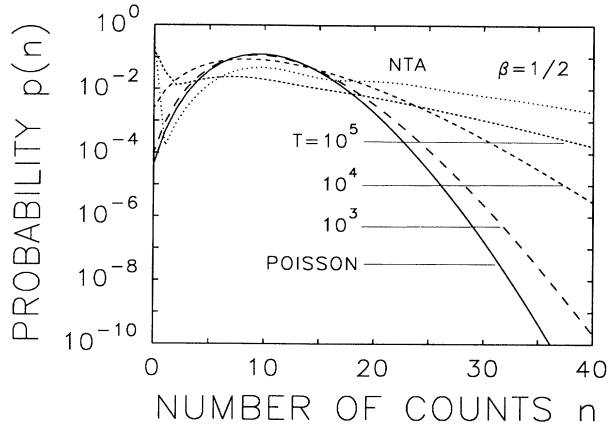

FIG. 3. Semilogarithmic plot of the counting distribution $p(n)$ vs count number n in Eqs. (16)–(18) for $\beta=\frac{1}{2}$ and three values of the counting time T: 10^3, 10^4, and 10^5. ($A=1$, $B=10^5$, $a=10$, $\langle n\rangle_n=10$.) For small values of the counting time T relative to the characteristic time τ_p, the distribution approaches the Poisson; for larger values it approaches the Neyman type A. Poisson and Neyman type-A distributions are included for comparison.

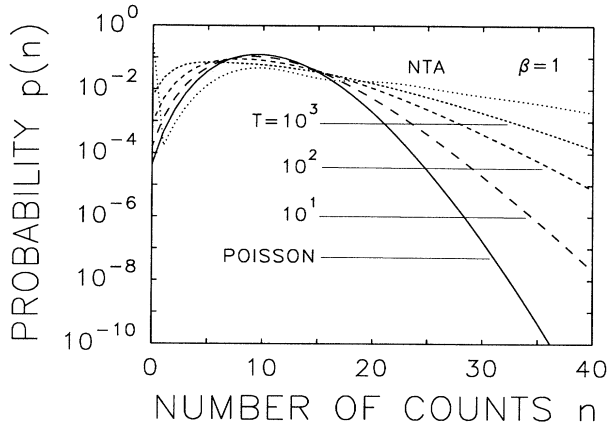

FIG. 4. Semilogarithmic plot of the counting distribution $p(n)$ vs count number n in Eqs. (16)–(18) for $\beta=1$ and three values of the counting time T: 10^1, 10^2, and 10^3. ($A=1$, $B=10^5$, $a=10$, $\langle n\rangle_n=10$.) For small values of the counting time T relative to the characteristic time τ_p, the distribution approaches the Poisson; for larger values it approaches the Neyman type A. Poisson and Neyman type-A distributions are included for comparison.

small, leading to the long counting time limit and the Neyman type-A distribution. This progression from Poisson to Neyman type-A distributions may be seen in the curves labeled "$T=10^3$" in Figs. 3–5.

2. Count moments

For the SNDP, the factorial moments, defined by

$$F_n^{(m)}\equiv\left\langle\prod_{i=0}^{m-1}(n-i)\right\rangle_n , \tag{22}$$

are given by the recurrence relation[6]

$$F_n^{(m+1)}=\sum_{i=0}^{m} b_i \begin{bmatrix} m \\ i \end{bmatrix} F_n^{(m-i)},\quad F_n^{(0)}\equiv 1 \tag{23}$$

where the coefficients b_i are defined by

$$b_i\equiv\mu\left\langle\int_{-\infty}^{\infty}[h_T(K,t)]^{i+1}dt\right\rangle . \tag{24}$$

The formulas for b_i for the FSNDP are provided in Appendix E. The standard moments $\langle n^m\rangle_n$ may be obtained from the factorial moments. In particular, the mean and variance are

$$\langle n\rangle_n=F_n^{(1)}=b_0=\mu\left\langle\int_{-\infty}^{\infty}h_T(K,t)dt\right\rangle=\mu T\left\langle\int_0^{\infty}h(K,t)dt\right\rangle=\mu aT , \tag{25}$$

$$\begin{aligned}\mathrm{var}[n]_n&=F_n^{(2)}+\langle n\rangle_n-\langle n\rangle_n^2=b_0+b_1=\mu aT+\mu\left\langle\int_{-\infty}^{\infty}[h_T(K,t)]^2dt\right\rangle\\&=\mu aT+2\mu\int_0^T(T-u)\left\langle\int_0^{\infty}h(K,t)h(K,t+u)dt\right\rangle du .\end{aligned} \tag{26}$$

3. Fano factor

The Fano factor F, defined as the ratio of the variance to the mean of a random variable, provides a measure of the variation a random variable exhibits with respect to the Poisson random variable, which has $F=1$.[28] Similarly, the Fano factor of a point process over a counting time T is the variance of the number of counts in an interval of duration T divided by the mean. Thus the Fano factor as a function of the counting time, also called the Fano-factor time curve, is defined as

$$F(T)\equiv\frac{\mathrm{var}[n]_n}{\langle n\rangle_n} . \tag{27}$$

For the homogeneous Poisson point process both the mean and the variance of the number of events in the process over a time interval T are equal to μT, so $F(T)$ is always unity for all rates μ and counting times T. More generally, the Fano factor varies with the counting time T.

For the SNDP Fano-factor calculations, we assume that the mean and variance integrals exist and are finite. In general, the Fano factor of the counting process, $N(t)$, is related to the Fano factor of the integrated-rate process, $W(t)$, by the simple relation

$$F(T)=1+\mathrm{var}[W]_W/\langle W\rangle_W . \tag{28}$$

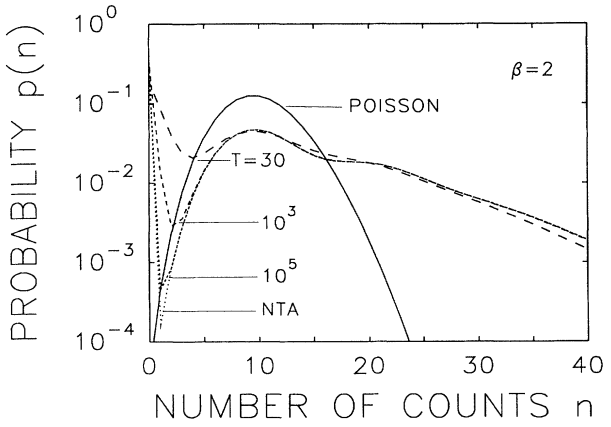

FIG. 5. Semilogarithmic plot of the counting distribution $p(n)$ vs count number n in Eqs. (16)–(18) for $\beta=2$ and three values of the counting time T: 30, 10^3, and 10^5. ($A=1$, $B=10^5$, $a=10$, $\langle n\rangle_n=10$.) For small values of the counting time T relative to the characteristic time τ_p, the distribution approaches the Poisson; for larger values it approaches the Neyman type A. Poisson and Neyman type-A distributions are included for comparison.

The Fano factor is then[6]

$$F(T)=1+\frac{2}{aT}\int_0^T(T-u)\times\left\langle\int_0^\infty h(K,t)h(K,t+u)dt\right\rangle du\ , \tag{29}$$

and, in particular, for the FSNDP we obtain

$$F(T)=1+\frac{2\langle K^2\rangle}{aT}\int_0^{\min(T,B-A)}(T-u)\times\int_A^{B-u}(t^2+ut)^{-\beta}dt\,du\ . \tag{30}$$

For any SNDP the Fano factor does not vary with the rate μ of the driving Poisson process, but generally varies with the counting time T.

Exact closed-form expressions for the FSNDP Fano factor do not exist except for certain values of the power-law exponent β. We calculate the Fano factor explicitly for the cases $\beta=\frac{1}{2}$ and $\beta=2$ and find approximations in the limit of small, medium, and large counting times T. Proofs and more detailed derivations are provided in Appendix F. For $\beta=\frac{1}{2}$ ($\alpha=1$) and $T\geq B-A$,

$$F=1+\frac{2\langle K^2\rangle}{3T\langle K\rangle}(3T-B+A)(B^{1/2}-A^{1/2})\ . \tag{31}$$

For $\beta=\frac{1}{2}$ ($\alpha=1$) and $T<B-A$,

$$F=1+\frac{\langle K^2\rangle}{3T\langle K\rangle(B^{1/2}-A^{1/2})}\times\left[3T^2\ln\left[\frac{B^{1/2}+(B-T)^{1/2}}{A^{1/2}+(A+T)^{1/2}}\right]-2(B^2-A^2)-(5T-2B)(B^2-BT)^{1/2}-(5T+2A)(A^2+AT)^{1/2}+6T(B+A)\right]\ . \tag{32}$$

For $\beta=2$ ($D=\frac{1}{2}$) and $T\geq B-A$,

$$F=1+\frac{\langle K^2\rangle}{AB(B-A)T\langle K\rangle}\times[T(B-A)^2+4AB(B-A)-2AB(B+A)\ln(B/A)]\ . \tag{33}$$

For $\beta=2$ ($D=\frac{1}{2}$) and $T<B-A$,

$$F=1+\frac{\langle K^2\rangle}{AB(B-A)T^2\langle K\rangle}\times[T^2(A^2+B^2)+2ABT(B-A)-2AB^2(A+T)\ln(1+T/A)-2A^2B(B-T)\ln(1-T/B)]\ . \tag{34}$$

For $T\ll A$, and for any B and β, the Fano factor approaches a form linear in T:

$$F(T)\approx 1+\frac{\langle K^2\rangle}{a}\left[\int_A^B t^{-2\beta}dt\right]T\ . \tag{35}$$

In the range $A\ll T\ll B$, the Fano factor approaches a simpler form which depends on β:

$$F(T)\approx 1+\frac{\langle K^2\rangle}{\langle K\rangle}\times\begin{cases}\dfrac{(1-\beta)}{(1-2\beta)}B^{-\beta}T, & 0\leq\beta<\frac{1}{2}\\ \frac{1}{2}B^{-1/2}[\ln(B/T)]T, & \beta=\frac{1}{2}\\ \dfrac{\Gamma(1-\beta)\Gamma(2\beta-1)}{(3-2\beta)\Gamma(\beta)}B^{\beta-1}T^{2(1-\beta)}, & \frac{1}{2}<\beta<1\\ \dfrac{\ln^2(T/A)}{\ln(B/A)}, & \beta=1\\ \dfrac{1}{(\beta-1)}A^{1-\beta}, & \beta>1\ .\end{cases} \tag{36}$$

For the range $\frac{1}{2}<\beta<1$ $(0<\alpha<1)$, the Fano factor depends on T in a power-law fashion, where the power-law exponent varies with β. Given in terms of $\alpha=2(1-\beta)$, the Fano factor becomes

$$F(T)\approx 1+\frac{\langle K^2\rangle\Gamma(\alpha/2)\Gamma(1-\alpha)}{\langle K\rangle(1+\alpha)\Gamma(1-\alpha/2)}B^{-\alpha/2}T^{\alpha} . \quad (37)$$

For $T\gg B$, and for any A and β, the Fano factor approaches the constant value

$$F(T)\approx 1+\frac{\langle K^2\rangle}{\langle K\rangle^2}a . \quad (38)$$

This is the Neyman type-A limit.

The excess Fano factor $F(T)-1$ as a function of the counting time T is shown in Fig. 6. The results are displayed in this manner because much of the power-law behavior in the Fano factor would be obscured by the constant unity term in the Fano-factor expression for the parameters used in the plot. For all graphs the impulse response function begins at $A=1$, ends at $B=10^6$, is deterministic, and has an area a equal to unity. For short counting times, in the range $T<A$, the excess Fano factor increases linearly with the counting time T, as provided in Eq. (35). As the counting time is increased, in the range $A\ll T\ll B$, the excess Fano factor varies in accordance with Eq. (36). For $\beta<\frac{1}{2}$ the excess Fano factor is still linear with T, and with $\beta=\frac{1}{2}$, the increase with T is slightly less than linear. For $\frac{1}{2}<\beta<1$, the excess Fano factor varies as $T^{\alpha}=T^{2(1-\beta)}=T^{1/2}$ in this example. While no clear functional relation is apparent for $\beta=1$, that provided in Eq. (36) is plausible. For $\beta=2$ the excess Fano factor is constant in this range of counting times. Finally, for large counting times $(T>B-A)$, the excess Fano factor is constant and equal to the area of the impulse response function (which in this case is unity), as provided by Eq. (38). Thus the excess Fano factor exhibits a range of power-law behavior with various power-law exponents over the range of counting times T.

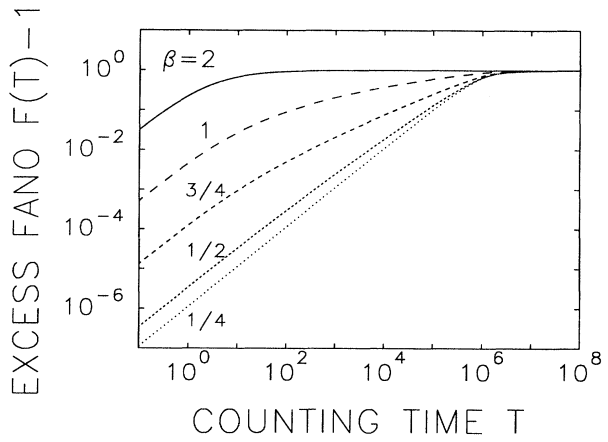

FIG. 6. Double logarithmic plot of the excess Fano factor $F(T)-1$ vs counting time T in Eq. (30) for five values of the power-law exponent β: $\frac{1}{4}$, $\frac{1}{2}$, $\frac{3}{4}$, 1, and 2 ($A=1$, $B=10^6$, $a=1$). The Fano factor exhibits a range of power-law behaviors as the counting time T and the power-law exponent β are varied, in accordance with Eqs. (35)–(38).

C. Normalized coincidence rate

The normalized coincidence rate $g^{(2)}(\tau)$ of a point process plays a role in time statistics analogous to that played by the Fano factor in count statistics; both functions are constant and equal to unity for a homogeneous Poisson process. It is related to the autocorrelation function used with continuous processes.[29] The normalized coincidence rate is a measure of the correlation between events with a specified time delay between them, regardless of intervening events. It is defined as[29]

$$g^{(2)}(\tau)\equiv\lim_{\Delta T\to 0}\frac{\Pr\{\mathcal{E}(\tau,\tau+\Delta T)\text{ and }\mathcal{E}(0,\Delta T)\}}{\Pr\{\mathcal{E}(\tau,\tau+\Delta T)\}\Pr\{\mathcal{E}(0,\Delta T)\}} . \quad (39)$$

where $\mathcal{E}(x,y)$ represents an event in the interval (x,y).

For finite, stationary point processes, the normalized coincidence rate may be obtained from the Fano factor by the relation[29]

$$g^{(2)}(\tau)=1+\frac{1}{2a}\frac{d^2}{dT^2}[TF(T)]\bigg|_{T=\tau} . \quad (40)$$

For the SNDP, the normalized coincidence rate is given by

$$g^{(2)}(\tau)=1+\frac{1}{\mu a^2}\left\langle\int_{-\infty}^{\infty}h(K,t)h(K,t+\tau)dt\right\rangle , \quad (41)$$

as shown in Appendix G. In particular, for the FSNDP,

$$g^{(2)}(\tau)=\begin{cases}1+\dfrac{\langle K^2\rangle}{\mu a^2}\displaystyle\int_A^{B-|\tau|}(t^2+|\tau|t)^{-\beta}dt, & |\tau|<B-A\\ 1, & |\tau|\geq B-A .\end{cases} \quad (42)$$

Closed-form expressions for the FSNDP coincidence rate do not exist except for certain values of the power-law exponent β. We solve for $g^{(2)}(\tau)$ in the three cases $\beta=\frac{1}{2}$, 1, and 2. Proofs for most of the expressions below may be adapted from those for power-law shot noise (Ref. 18, Appendix D), since the forms of the coincidence rate for the FSNDP and those for the autocorrelation function for power-law shot noise are linearly related. The exception is the case $A\ll\tau\ll B$ and $\beta>1$, which is considered in Appendix G.

For $\beta=\frac{1}{2}$ $(\alpha=1)$,

$$g^{(2)}(\tau)=\begin{cases}1+2\dfrac{\langle K^2\rangle}{\mu a^2}\ln\left[\dfrac{B^{1/2}+(B-|\tau|)^{1/2}}{A^{1/2}+(A+|\tau|)^{1/2}}\right], & 0\leq|\tau|<B-A\\ 1, & |\tau|\geq B-A .\end{cases} \quad (43)$$

For $\beta=1$,

$$g^{(2)}(\tau)=\begin{cases}1+\dfrac{\langle K^2\rangle}{\mu a^2}(A^{-1}-B^{-1}), & \tau=0\\ 1+\dfrac{\langle K^2\rangle}{\mu a^2|\tau|}\ln[(1-|\tau|/B)(1+|\tau|/A)], & 0<|\tau|<B-A\\ 1, & |\tau|\geq B-A\ .\end{cases} \tag{44}$$

For $\beta=2$ ($D=\frac{1}{2}$),

$$g^{(2)}(\tau)=\begin{cases}1+\dfrac{\langle K^2\rangle}{3\mu a^2}(A^{-3}-B^{-3}), & \tau=0\\ 1+\dfrac{\langle K^2\rangle}{\mu a^2}\left[\dfrac{2A+|\tau|}{|\tau|^2A(A+|\tau|)}-\dfrac{2B-|\tau|}{|\tau|^2B(B-|\tau|)}+\dfrac{2}{|\tau|^3}\ln[(1-|\tau|/B)(1+|\tau|/A)]\right], & 0<|\tau|<B-A\\ 1, & |\tau|\geq B-A\ .\end{cases} \tag{45}$$

For small delay times τ, and for any power-law exponent β, the normalized coincidence rate approaches a constant value

$$g^{(2)}(\tau)=1+\frac{\langle K^2\rangle}{\mu a^2}\int_A^B t^{-2\beta}dt\ . \tag{46}$$

In the region $A\ll|\tau|\ll B$, the normalized coincidence rate approaches a simpler form which depends on β. In that case,

$$g^{(2)}(\tau)=1+\frac{\langle K^2\rangle}{\mu\langle K\rangle^2}\times\begin{cases}\dfrac{(1-\beta)^2}{(1-2\beta)}B^{-1}, & 0\leq\beta<\frac{1}{2}\\ \frac{1}{4}B^{-1}\ln(B/|\tau|), & \beta=\frac{1}{2}\\ \dfrac{(1-\beta)\Gamma(2-\beta)\Gamma(2\beta-1)}{\Gamma(\beta)}B^{2\beta-2}|\tau|^{1-2\beta}, & \frac{1}{2}<\beta<1\\ \dfrac{\ln(|\tau|/A)}{\ln^2(B/A)}|\tau|^{-1}, & \beta=1\\ (\beta-1)A^{\beta-1}|\tau|^{-\beta}, & \beta>1\ .\end{cases} \tag{47}$$

In the range $\frac{1}{2}<\beta<1$ ($0<\alpha<1$), the normalized coincidence rate depends on τ in a decaying power-law fashion, where the power-law exponent varies with β. Given in terms of α, the coincidence rate becomes

$$g^{(2)}(\tau)=1+\frac{\alpha\langle K^2\rangle\Gamma(1+\alpha/2)\Gamma(1-\alpha)}{2\mu\langle K\rangle^2\Gamma(1-\alpha/2)}B^{-\alpha}|\tau|^{\alpha-1}\ . \tag{48}$$

For all $\beta<1$, the normalized coincidence-rate dependence on T differs from that of the Fano factor by a constant T^1—that is, if $F(T)-1\propto T^\alpha$, then $g^{(2)}(\tau)-1\propto\tau^{\alpha-1}$. If $\beta\geq1$, then the impulse response function has infinite area near the onset time A in the limit $A\to0$, so Eq. (40) does not apply.

The excess normalized coincidence rate $g^{(2)}(\tau)-1$, as a function of delay time τ, is shown in Fig. 7. As with the Fano factor, we graph excess values to highlight the power-law dependencies in the coincidence rates. For all graphs the impulse response function begins at $A=1$ and ends at $B=5\times10^6$, and the rate μ of the primary Poisson process $M(t)$ is equal to unity. For short delay times the excess normalized coincidence rate is constant, as provided in Eq. (46). This holds approximately for $|\tau|<A$. As the counting time is increased, in the range $A\ll|\tau|\ll B$ the excess normalized coincidence rate varies in accordance with Eq. (47). For $0<\beta<\frac{1}{2}$ the excess normalized coincidence rate is still constant with τ, whereas with $\beta=\frac{1}{2}$, it decreases slightly with τ. For $\frac{1}{2}<\beta<1$, the excess normalized coincidence rate varies as $|\tau|^{1-2\beta}=|\tau|^{\alpha-1}$—that is, as $|\tau|^{-1/2}$ in this example. For $\beta=1$, the excess normalized coincidence rate decreases slightly more slowly than $1/|\tau|$, and for $\beta>1$ it varies as $|\tau|^{-\beta}$. Finally, for delay times larger than $B-A$, the excess normalized coincidence rate is zero. Thus, like the Fano factor, the excess normalized coincidence rate also exhibits a range of power-law behavior with various power-law exponents over the range of delay times τ.

D. Power spectral density

The power spectral density $S_N(f)$ of the FSNDP is obtained with the help of the Wiener-Khintchin theorem. The Fourier transform of the coincidence rate in Eq. (42) is

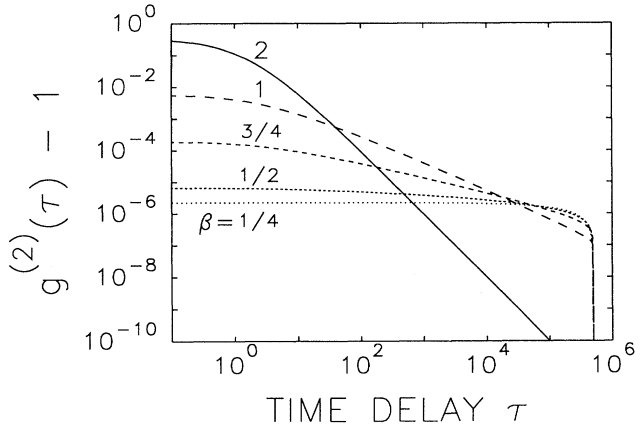

FIG. 7. Double logarithmic plot of the excess normalized coincidence rate $g^{(2)}(\tau)-1$ vs delay time τ in Eq. (42) for five values of the power-law exponent β: $\frac{1}{4}$, $\frac{1}{2}$, $\frac{3}{4}$, 1, and 2 ($A=1$, $B=5\times10^5$, $\mu=1$). The autocorrelation functions exhibit approximate power-law behavior with various exponents for a good portion of their range, in accordance with Eq. (47). Note the abrupt decrease in $g^{(2)}(\tau)-1$ near $\tau=B-A=5\times10^5$, at which point $g^{(2)}(\tau)$ becomes unity.

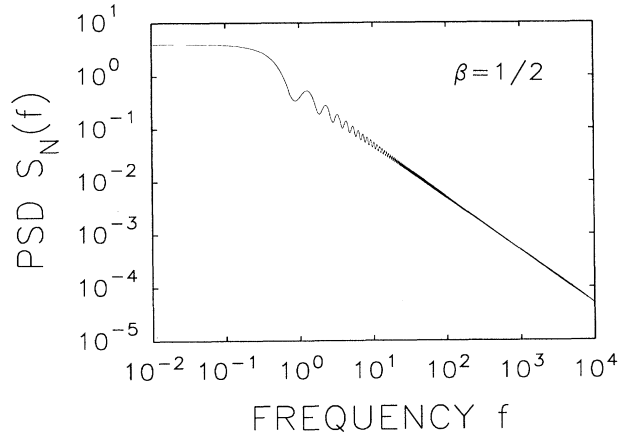

FIG. 8. Double logarithmic plot of the power spectral density $S_N(f)$ vs frequency f for $\beta=\frac{1}{2}$ ($A=0$, $B=1000$). Note that the power spectral density exhibits $1/f^{\alpha}$ behavior with exponent $\alpha=1$ for high frequencies and that the abrupt cutoff in the impulse response function gives rise to oscillations in the frequency domain.

$$S_N(f)=\delta(f)+\frac{\langle K^2\rangle}{\mu a^2}|\Gamma(1-\beta,j2\pi fA) - \Gamma(1-\beta,j2\pi fB)|^2(2\pi f)^{2\beta-2} , \tag{49}$$

where $\Gamma(\ ,\ )$ is the incomplete gamma function defined by

$$\Gamma(a,x)\equiv\int_x^{\infty} e^{-t}t^{a-1}dt . \tag{50}$$

For the case when $\beta<1$ ($\alpha>0$), $A=0$, and B is finite, the above form reduces to

$$\begin{aligned} S_N(f)&=\delta(f)+\frac{\langle K^2\rangle}{\mu a^2}|\Gamma(1-\beta)-\Gamma(1-\beta,j2\pi fB)|^2 \times(2\pi f)^{2\beta-2} \\ &=\delta(f)+\frac{\langle K^2\rangle}{\mu a^2}|\Gamma(\alpha/2)-\Gamma(\alpha/2,j2\pi fB)|^2 \times(2\pi f)^{-\alpha} . \end{aligned} \tag{51}$$

In the limit $f\to0$ the spectrum approaches the constant value $\langle K^2\rangle/\mu\langle K\rangle^2$ by the definition of the Fourier transform, and in the limit $f\to\infty$ the incomplete gamma function approaches zero, yielding

$$S_N(f)\to\frac{\Gamma^2(1-\beta)\langle K^2\rangle}{\mu a^2(2\pi)^{\alpha}}f^{-\alpha} . \tag{52}$$

Thus the FSNDP can serve as a source of generalized impulsive $1/f$ noise, and the power spectral density has the same form as that of fractal shot noise.[16,18] This is expected, since the last stage of the SNDP model is a Poisson transform, which does not alter the power spectral density of a process.

Figure 8 shows the shot-noise power spectral densities obtained with $\alpha=1$ ($\beta=\frac{1}{2}$) with $A=0$ and $B=1000$. The power spectral density takes the form $1/f$ for high frequencies. Note that the abrupt cutoff in the time domain gives rise to oscillations in the frequency domain.

E. Time statistics

A point process may also be reduced to a single random number by considering the relative times associated with event occurrences. The most important of these is the interevent time, defined as the time between adjacent events. The forward recurrence time, the time to the next event from a random starting time (chosen independently of the point process), is also important. Both of these random times may be described in terms of their probability densities, moments, and other statistical parameters, as with number statistics. For the homogeneous Poisson process, both the forward recurrence and interevent times have exponential probability densities with mean values equal to the reciprocal of the rate of the process.

The forward recurrence and interevent time probability densities, denoted $P_1(\tau)$ and $P_2(\tau)$, respectively, are given below. We begin with the probability of observing no events in a SNDP in a time interval of length τ, which is $\Pr\{n=0\}$ from Eq. (18),

$$\begin{aligned} P_0(\tau)&=p(0) \\ &=Q_W(1) \\ &=\exp\left[\mu\left\langle\int_{-\infty}^{\infty}\{\exp[-h_{\tau}(K,u)]-1\}du\right\rangle\right] . \end{aligned} \tag{53}$$

The forward recurrence time has a probability density function given by the rate at which the probability of observing zero events decreases:

$$P_1(\tau)=-\frac{d}{d\tau}P_0(\tau)$$
$$=-\frac{d}{d\tau}\exp\left[\mu\left\langle\int_{-\infty}^{\infty}\{\exp[-h_\tau(K,u)]-1\}du\right\rangle\right]. \tag{54}$$

The probability density function for the interevent time is the normalized rate of change of the above value and is given by

$$P_2(\tau)=-\frac{1}{\langle I\rangle_I}\frac{d}{d\tau}P_1(\tau)$$
$$=\frac{1}{\mu a}\frac{d^2}{d\tau^2}\exp\left[\mu\left\langle\int_{-\infty}^{\infty}\{\exp[-h_\tau(K,u)]-1\}du\right\rangle\right], \tag{55}$$

where $I(t)$ is the shot-noise process at the output of the linear filter (see Fig. 1). The formulas for $P_0(\tau)$, $P_1(\tau)$, and $P_2(\tau)$ for the FSNDP are listed in Appendix E. For $\tau=0$ we have

$$P_1(0)=1/\langle\tau\rangle_\tau,$$
$$P_2(0)=1/\langle\tau\rangle_\tau+\langle\tau\rangle_\tau \mathrm{var}[I]_I. \tag{56}$$

In the limit $\tau\to\infty$, both probability density functions approach an exponential form

$$P_1(\tau)\to\mu(1-e^{-a})\exp[-\mu\tau(1-e^{-a})],$$
$$P_2(\tau)\to\frac{\mu(1-e^{-a})^2}{a}\exp[-\mu\tau(1-e^{-a})]. \tag{57}$$

Probability density functions for forward recurrence times are shown in Figs. 9 and 11, while those for interevent times are displayed in Figs. 10 and 12. In all cases the power-law impulse response function $h(t)$ begins at $A=1$ and ends at $B=10^5$, and each figure is parametrized by the power-law exponent β. For Figs. 9 and 10 the rate μ of the primary Poisson process $M(t)$ is 10^{-4} and for all the impulse response functions the area a is 100, yielding an expected interevent time $\langle\tau\rangle_\tau$ for $N(t)$ of 100. For Figs. 11 and 12, the corresponding values are

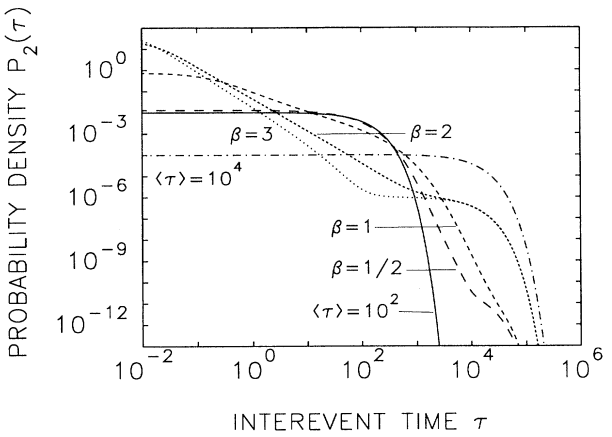

FIG. 10. Double logarithmic plot of the interevent time probability density function $P_2(\tau)$ vs τ in Eq. (55) for four values of the power-law exponent β, labeled $\beta=\frac{1}{2}$, $\beta=1$, $\beta=2$, and $\beta=3$. The degree of overlap is 10 ($A=1$, $B=10^5$, $a=100$, $\langle\tau\rangle_\tau=100$, $\mu=10^{-4}$). Exponential distributions with mean values of 100 and 10^4, labeled $\langle\tau\rangle=10^2$ and $\langle\tau\rangle=10^4$, are included for comparison. The probability density exhibits a wide range of power-law behaviors as the time τ and the power-law exponent β are varied.

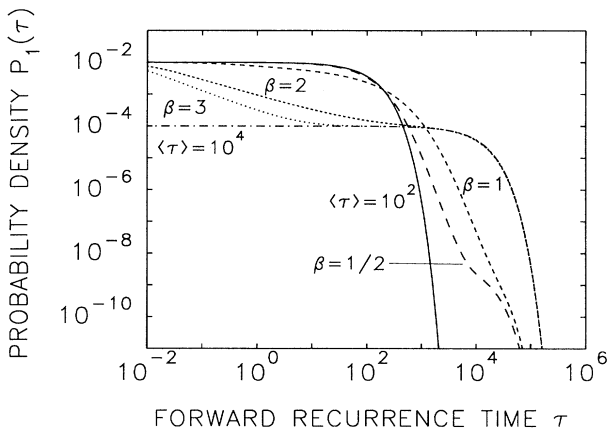

FIG. 9. Double logarithmic plot of the forward recurrence time probability density function $P_1(\tau)$ vs τ in Eq. (54) for four values of the power-law exponent β, labeled $\beta=\frac{1}{2}$, $\beta=1$, $\beta=2$, and $\beta=3$. The degree of overlap is 10 ($A=1$, $B=10^5$, $a=100$, $\langle\tau\rangle_\tau=100$, $\mu=10^{-4}$). At time limits short compared to the characteristic time τ_p the distributions approach an exponential form with a mean value of 100. Exponential distributions with mean field values of 100 and 10^4, labeled $\langle\tau\rangle=10^2$ and $\langle\tau\rangle=10^4$, are included for comparison.

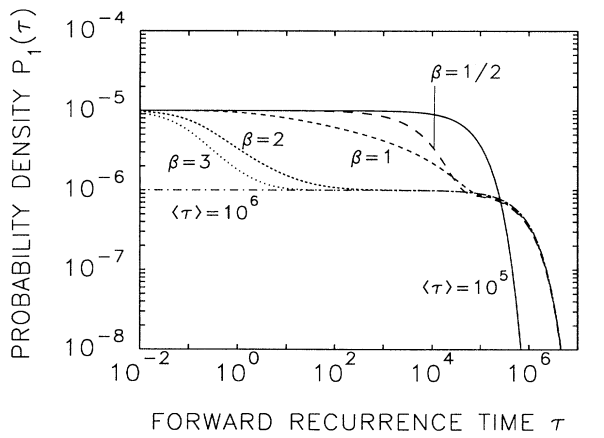

FIG. 11. Double logarithmic plot of the forward recurrence time probability density function $P_1(\tau)$ vs τ in Eq. (54) for four values of the power-law exponent β, labeled $\beta=\frac{1}{2}$, $\beta=1$, $\beta=2$, and $\beta=3$. The degree of overlap is 0.1 ($A=1$, $B=10^5$, $a=10$, $\langle\tau\rangle_\tau=10^5$, $\mu=10^{-6}$). At time limits short compared to the characteristic time τ_p, the distributions approach an exponential form with a mean value of 10^5. Exponential distributions with mean values of 10^5 and 10^6, labeled $\langle\tau\rangle=10^5$ and $\langle\tau\rangle=10^6$, are included for comparison.

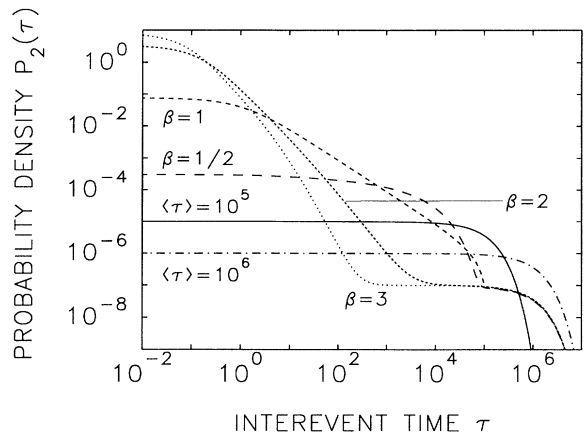

FIG. 12. Double logarithmic plot of the interevent time probability density function $P_2(\tau)$ vs τ in Eq. (55) for four values of the power-law exponent β, labeled $\beta=\frac{1}{2}$, $\beta=1$, $\beta=2$, and $\beta=3$. The degree of overlap is 0.1 ($A=1$, $B=10^5$, $a=10$, $\langle\tau\rangle_\tau=10^5$, $\mu=10^{-6}$). Exponential distributions with mean values of 10^5 and 10^6, labeled $\langle\tau\rangle=10^5$ and $\langle\tau\rangle=10^6$, are included for comparison. The probability density exhibits a wide range of power-law behaviors as the time τ and the power-law exponent β are varied.

$\mu=10^{-6}$, $a=10$, and $\langle\tau\rangle_\tau=10^5$. Exponential density functions with mean values equal to $1/\mu$ and $\langle\tau\rangle_\tau$ are included in all figures for comparison.

Significant differences among the various curves in Figs. 9–12 result from the varying amounts of clustering exhibited by the FSNDP. A large degree of clustering increases the probability of very short and very long interevent times at the expense of times near the mean value, when compared with an exponential density of the same mean value. Such clustering derives from variations in the fractal shot-noise rate $I(t)$, and in Figs. 9–12 depends explicitly on two factors. Increasing the power-law exponent β increases the clustering. For larger β, particularly $\beta>1$, most of the area a of the impulse response function is concentrated in the small region near the onset A, with proportionately less area in the tail. For smaller β, the value of the impulse response function does not change as much over its duration $B-A$. Thus the shot-noise rate $I(t)$ exhibits more variation, and the FSNDP exhibits more clustering for large values of β, all other parameters being held constant.

The degree of overlap of the impulse response functions also contributes to the clustering when $\beta<1$. For $\mu(B-A)\ll 1$, the expected time between events of the primary Poisson process $M(t)$ is $1/\mu$, which far exceeds the duration of the impulse response function, which is $B-A$. Thus successive contributions to Eq. (1) will rarely overlap. Then $I(t)$ will be positive only for relatively short intervals ($B-A$) separated by much longer intervals ($1/\mu$) during which it will be zero, and the events $dN(t)$ of the FSNDP will be restricted to those relatively shorter intervals, thereby leading to clustering. If $\mu(B-A)\gg 1$, however, the successive contributions to Eq. (1) will tend to overlap, resulting in a smoothing of the variation in amplitude seen in the individual impulse response functions. Indeed, the coefficient of variation of I, defined as the standard deviation divided by the mean, varies as $\mu^{-1/2}$. For $\beta>1$, however, the tail of the impulse response function has little area, and whether or not it overlaps another impulse response function is much less important. In Figs. 9 and 10 the degree of overlap $\mu(B-A)$ is 10, while in Figs. 11 and 12 it is 0.1.

The forward recurrence time and interevent time probability density functions of the FSNDP exhibit various kinds of behavior over the range of times τ. Starting at $\tau=0$, we have $P_1(0)=1/\langle\tau\rangle_\tau$, which is constant with β, but

$$P_2(0)=1/\langle\tau\rangle_\tau+\langle\tau\rangle_\tau \mathrm{var}[I]_I \ ,$$

which increases with β, reflecting the increased clustering for larger β. This effect is enhanced in Fig. 12, where the degree of overlap is much smaller than in Fig. 10. For small times τ compared with the characteristic time τ_p, and small power-law exponents β, $P_1(\tau)$ follows an exponential density of the same mean, since over this short time scale the intensity $I(t)$ appears relatively constant. Agreement with the exponential density is closer for smaller β. Similarly, for small β the interevent time probability density $P_2(\tau)$ also follows an exponential form for small times τ. The mean of the approximated exponential density is higher, reflecting the conditional intensity $I(t)$; given that an event has just occurred, the instantaneous rate is likely to be increased, since $P_2(0)>P_1(0)$.

For large times τ the effects of the primary Poisson process $M(t)$ become important. For $\beta>1$, the area of the impulse response functions a being concentrated near the onset time A causes the events $dN(t)$ of the FSNDP to be clustered tightly after the primary events. Thus the long intervals are essential those of the primary process $M(t)$, and $P_1(\tau)$ follows an exponential density with associated mean $1/\mu$. The interevent time probability density $P_2(\tau)$ follows the same exponential form, but with values decreased by a factor equal to the area of the impulse response function a. Each primary event $dM(t)$ gives rise to a number of secondary events, and therefore an equal number of intervals, with mean number equal to the area of the impulse response function a, only one of which is the long interval before the next primary event. In Figs. 11 and 12 the degree of overlap is so small that long intervals during which the shot-noise rate $I(t)=0$ are common. At these times no events are possible in the SNDP. Here the form of the impulse response function is not important, and all converge to an exponential form associated with the primary Poisson process for times $\tau>B-A$. Finally, for large times ($\tau\gg B-A$), regardless of the impulse response function shape or primary process rate μ, both $P_1(\tau)$ and $P_2(\tau)$ approach the exponential forms given by Eq. (57).

F. Gaussian FSNDP

Under suitable conditions, the underlying power-law shot noise $I(t)$ converges to a Gaussian probability density, and therefore the resulting process $N(T)$ will be a Gaussian-driven FSNDP. This is important because Gaussian processes are ubiquitous, well understood, and

may be completely described by their means and autocovariance functions. The process $I(t)$ will approach a Gaussian amplitude density in the limit $\mu \to \infty$ if $\langle K^n \rangle < \infty$ for all n, $A > 0$, and $B < \infty$ for $\beta \leq 1$,[18] as provided by the central limit theorem. Indeed, expansions about the Gaussian density quantify the approach to the Gaussian limit as μ, the rate of the primary process $M(t)$, increases without bound.[18] Furthermore, the resulting FSNDP will not have trivial properties, and in particular will not approach the HPP limit. The Fano factor of $N(t)$, for example, will not change as μ increases; expressions for the Fano factor $F(T)$ in Eqs. (29)–(38) do not involve μ. Thus suitable parameters β, A, B, K, and μ may be chosen to obtain an amplitude probability density for I which follows the Gaussian arbitrarily closely and simultaneously deviates from the HPP by any desired amount. In this case the FSNDP closely approximates a fractal-Gaussian-driven DSPP and may be completely defined by the corresponding mean and autocovariance function[18]

$$\begin{aligned} \langle I \rangle_I &= \mu a = \langle K \rangle \int_A^B t^{-\beta} dt \ , \\ \mathrm{cov}[\tau]_I &= \langle K^2 \rangle \int_A^{B-|\tau|} (t^2 + |\tau| t)^{-\beta} dt \ , \end{aligned} \tag{58}$$

which indeed exhibits power-law behavior over a wide range of times τ.

V. APPLICATIONS

The FSNDP provides a well-defined framework modeling a number of physical processes. In this section we apply our model to two areas: Cherenkov radiation resulting from the motion of a random stream of charged particles, and diffusion of randomly injected concentration packets. In Cherenkov radiation, the particles induce fields with power-law decay characteristics, which in turn emit photons. In diffusion, the concentration of a substance diffuses away from an initial location as a decaying power-law function of time, and secondary events may be generated in proportion to this concentration.

A. Cherenkov radiation from a random stream of charged particles

Charged particles traveling faster than the group velocity of light in a transparent medium emit photons, often in the visible range. This phenomenon was first examined systematically in a series of experiments conducted by Cherenkov beginning in 1934. We use semiclassical electromagnetic theory to show that the photons produced by Cherenkov radiation, arising from a random stream of charged particles, may be modeled by the FSNDP.

Consider a charged particle traveling along the positive x axis through a transparent, nonferromagnetic medium of refractive index n, at a speed $v > c/n$, as shown in Fig. 13. We define the quantity $J \equiv [(nv/c)^2 - 1]^{1/2}$, which is a function of the amount by which the particle velocity exceeds the Cherenkov limit $v = c/n$. The electric and magnetic fields are calculated at a distance d from the x axis, where the arbitrary point in the x-z plane $\{-Jd, 0, d\}$ is chosen for algebraic simplicity. We assume that the particle does not experience substantial deceleration while it is significantly close to this observation point. Following Jelley[30] and Zrelov,[31] we obtain scalar and vector potentials satisfying the Lorentz gauge condition

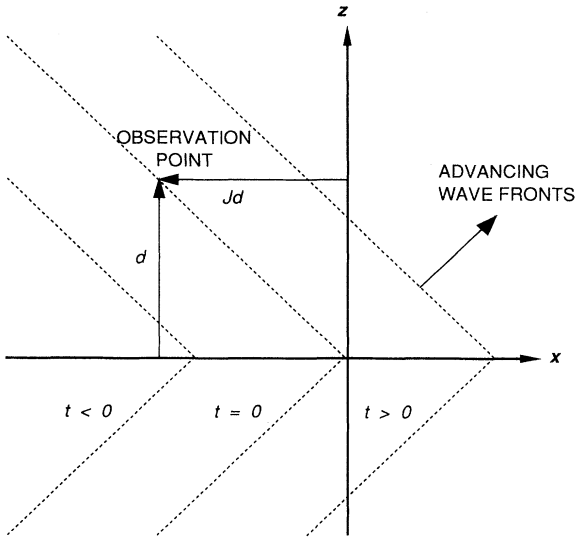

FIG. 13. A charged particle moving faster than the speed of light in a medium emits Cherenkov radiation. At the point $\{-Jd, 0, d\}$, the photon flux density will decay as an inverse power-law function of time. Wave fronts are shown for a particle traveling along the x axis at $t < 0$, $t = 0$, and $t > 0$.

$$\phi = 2qn^{-2}[(x - vt)^2 - J^2(y^2 + z^2)]^{-1/2} \ , \tag{59}$$

$$\mathbf{A} = \frac{n^2}{c} \mathbf{v} \phi \ , \tag{60}$$

respectively, where q is the charge of the particle.

The corresponding electric field is

$$\begin{aligned} \mathbf{E} &= -\nabla\phi - \frac{1}{c} \frac{\partial \mathbf{A}}{\partial t} \\ &= -\frac{2qJ^2}{n^2} [(x - vt)^2 - J^2(y^2 + z^2)]^{-3/2} \{x - vt, y, z\} \\ &= \frac{2qJ^2}{n^2} [(vt)^2 + 2Jdvt]^{-3/2} \{(vt + Jd), 0, -d\} \\ &= \frac{2qJ^2}{n^2 v^2} [t^2 + 2t_1 t]^{-3/2} \{t + t_1, 0, -d/v\} \ , \end{aligned} \tag{61}$$

where

$$t_1 \equiv Jd/v = d(n^2 c^{-2} - v^{-2})^{1/2} \ .$$

For a nonferromagnetic medium,

$$\mathbf{H}=\mathbf{B}=\nabla\times\mathbf{A}$$
$$=\frac{2qv}{c}[(x-vt)^2-J^2(y^2+z^2)]^{-3/2}\{0,J^2z,-J^2y\}$$
$$=\frac{2qdvJ^2}{c}[(vt)^2+2Jdvt]^{-3/2}\{0,1,0\}$$
$$=\frac{2qdJ^2}{cv^2}[t^2+2t_1t]^{-3/2}\{0,1,0\}\ . \tag{62}$$

The foregoing is valid for times when the quantities in the square brackets in Eqs. (61) and (62) are positive—namely, for $t>0$. For $t<0$ the electromagnetic shock wave generated by the particle has not yet reached the observation point, so that all fields are zero and there are no photons. The energy flux density and its direction are determined by the Poynting vector

$$\mathbf{S}\equiv\frac{c}{4\pi}\mathbf{E}\times\mathbf{H}$$
$$=\frac{c}{4\pi}\frac{2qJ^2}{n^2v^2}\frac{2qdJ^2}{cv^2}[t^2+2t_1t]^{-3}\{t+t_1,0,-d/v\}$$
$$\times\{0,1,0\}$$
$$=\frac{q^2dJ^4}{\pi n^2v^4}[t^2+2t_1t]^{-3}\{d/v,0,t+t_1\}\ . \tag{63}$$

The magnitude of the Poynting vector is

$$|\mathbf{S}|=\frac{q^2dn^2J^4}{\pi v^4}[t^2+2t_1t]^{-3}$$
$$\times[t^2+2t_1t+t_1^2+(d/v)^2]^{1/2}$$
$$=\frac{q^2dn^2J^4}{\pi v^4}[t^2+2t_1t]^{-3}[t^2+2t_1t+(nd/v)^2]^{1/2}$$
$$=\frac{q^2dn^2J^4}{\pi v^4}[t^2+2t_1t]^{-3}[t^2+2t_1t+t_2^2]^{1/2}\ , \tag{64}$$

where $t_2\equiv nd/c$. The light will have a spectrum which may be calculated by Fourier transform methods,[30,31] or from Eq. (49). If we define $\bar{\nu}$ to be the average frequency of the light, then the photon flux density as a function of time may be approximated as

$$h(t)\approx|\mathbf{S}|/h\bar{\nu}\ . \tag{65}$$

This photon-flux-density time function may be cast in the form of a simple power-law impulse response function as in Eq. (2). The magnitude of the Poynting vector, and therefore the photon flux density, exhibits power-law decay with a power-law exponent that increases at the crossover time $t=t_1$, and decreases at time $t=t_2$. No real medium will pass frequency components of arbitrarily high frequency, and indeed all systems have practical limits to the frequency components which may be observed at the output. The difference between the upper and lower frequency limits is the system bandwidth $\Delta\nu$. Similarly, the onset time of the light pulse will be limited to a value roughly equal to the inverse of the bandwidth; we define $t_0\equiv1/\Delta\nu$. In addition, the nonzero size of the charged particle imposes a limit on the onset time,[31] although this limit will be relatively unimportant since we can assume that the particle is smaller than the wavelength of the generated photons.

The photon-flux-density time function $h(t)$ exhibits a range of power-law exponents as the time t increases. For times larger than the onset time t_0, but still less than t_1, $h(t)$ will decay approximately as a simple power law with exponent $\beta=3$. For $t_1<t<t_2$, $h(t)$ decays more rapidly, with $h(t)\sim t^{-6}$. Finally, for $t>t_2$, $h(t)$ will decay as t^{-5}. Thus,

$$h(t)\sim\begin{cases}0, & t<t_0\\ t^{-3}, & t_0<t<t_1\\ t^{-6}, & t_1<t<t_2\\ t^{-5}, & t>t_2\ .\end{cases} \tag{66}$$

Even for relatively narrow bandwidths, the onset time t_0 will often be several orders of magnitude smaller than t_1, ensuring a large range of times for which t^{-3} behavior is observed. In the wavelength range 536 to 556 nm, as studied by Cherenkov in 1938 for example, the onset time is calculated to be $t_0\approx50$ fs. Particles traveling close to the speed of light through materials with a refractive index as low as 1.2, with d as small as 1 cm to the observation point, yield a crossover time $t_1\approx22$ ps. Most media will have much larger bandwidths, and correspondingly more of a difference between t_0 and t_1. For such particles we can make the approximation that $h(t)=0$ for $t<t_0$, and similarly $h(t)=0$ for $t>t_1$, since the power-law decay exponent increases at $t=t_1$. The energy-flow time-response functions due to a single charged particle emitting Cherenkov radiation may then be closely approximated by

$$h(t)\approx\begin{cases}Kt^{-3}, & A<t<B\\ 0, & \text{otherwise}\ ,\end{cases} \tag{67}$$

where we identify $A=t_0$ and $B=t_1$.

In media whose index of refraction differs only slightly from unity, the power-law crossover time t_1 of the impulse response function $h(t)$ will be very small, possibly smaller than the onset time t_0. In that case $h(t)$ will lack the t^{-3} portion and will be of the form

$$h(t)\approx\begin{cases}Kt^{-5}, & t>t_0\\ 0, & \text{otherwise}\ .\end{cases} \tag{68}$$

However, since the energy production is proportional to J^4, if the index of refraction differs only slightly from unity, then J will be small and the total light energy will be small, thereby reducing the overall number of emitted photons.

Thus a single particle gives rise to a photon flux density that follows a decaying power-law time function. If a number of particles travel along the x axis, they will stimulate independent sets of photons, as long as these particles are separated by a sufficient time interval so that their respective electric and magnetic fields do not overlap significantly. Since the form of the Poynting vector involves a vector multiplication, cross products between the two sets of fields will appear, and the resulting sequence of photon generations will not be a simple linear superposition of the photon generations that would result

from the two particles had they arrived separately. Radioactive sources, such as alpha emitters and beta emitters, and particle accelerators operated at low current levels, generate Poisson time sequences of energetic charged particles with essentially identical positions and velocities. When these particles pass through a transparent medium under the conditions mentioned above, the point process resulting from the generated Cherenkov photon events will obey the FSNDP model.

B. Diffusion of randomly injected concentration packets

Diffusion provides a broad area of applicability for the FSNDP model. In classical diffusion, particle concentrations decrease in a power-law fashion. Consider a concentration U_0 of infinitesimal particles, all initially at some point $\mathbf{x}=\mathbf{x}_0$ of a d-dimensional space ($d<4$), at starting time $t=0$. Then the concentration at $\mathbf{x}=0$ at some later time t will be represented by a Gaussian density with a variance that increases with time in a power-law fashion,[32]

$$U(t)=U_0(4\pi t\Delta)^{-d/2}\exp\left[-\frac{|\mathbf{x}_0|^2}{4t\Delta}\right]$$
$$=K_0\exp(-t_0/t)t^{-d/2}\,, \tag{69}$$

where $K_0\equiv U_0(4\pi\Delta)^{-d/2}$, $t_0\equiv|\mathbf{x}_0|^2/4\Delta$, and Δ is the diffusion constant. Except for a rapidly decaying transient near $t=0$, negligible when $t>5t_0$, the concentration $U(t)$ varies as $t^{-d/2}$ and thus decays as a power-law function. We assume that the particles have some lifetime t_1, resulting in $U(t)\approx 0$ for $t>t_1$. If secondary events are generated proportionally to the local concentration of particles, then the generation rate may be identified as the impulse response function

$$h(t)\approx\begin{cases}K_0t^{-d/2}, & A<t<B\\ 0, & \text{otherwise}\,,\end{cases} \tag{70}$$

where $A=t_0$ and $B=t_1$. Finally, if new packets of concentration are deposited at $\mathbf{x}_0$ at Poisson times, the secondary event process will be accurately modeled by the FSNDP. In general, the packets may arrive at points $\mathbf{x}\neq\mathbf{x}_0$ for some processes, and they need not all have the same initial concentration U_0. The FSNDP model is readily applied to this general case by using stochastic K instead of deterministic K_0 in the impulse response function. Thus diffusion yields a rich area of applicability for the FSNDP, particularly with exponents $\beta=\frac{1}{2}$, 1, and $\frac{3}{2}$, corresponding to diffusion in one, two, and three dimensions, respectively. In particular, for the case $\beta=\frac{1}{2}$, the power spectral density will be precisely $1/f$; thus diffusion in one dimension can give rise to a $1/f$-type spectrum. Other values of β may also be applicable if the particles are constrained to remain on a fractal set or are of two species which combine in pairs of opposite type.

1. *Semiconductor high-energy particle detectors*

Diffusion and the FSNDP are also important in describing the behavior of semiconductor high-energy particle detectors. A typical detector consists of a lightly doped p-n junction across which a large reverse bias is applied.[33] Energetic charged particles enter the detector, usually along the p-n axis, and create electron-hole pairs within a large part of the semiconductor depletion region. The higher the energy of the particle, the greater the number of electron-hole pairs produced. These carriers are then swept out of the depletion region of the diode by the high reverse-bias field, electrons toward the n region and holes towards the p region. This occurs before many of the electrons and holes recombine. However, some of the carriers do recombine, reducing the detected charge created by the original energetic charged particle, so a description of the recombination process is useful.

Consider a single energetic particle entering the detector at a time $t=0$. We assume that the electron-hole pairs are created instantaneously throughout the semiconductor depletion region, distributed in a three-dimensional Poisson fashion, and that they begin diffusing as soon as they are created. Whenever an electron and a hole approach within some critical radius, the two carriers either annihilate each other immediately or first form an exciton and later recombine. In either case they no longer carry current and may be considered to be annihilated. For now we ignore the drift current; later we will consider the case where drift current is important.

The solution to this semiconductor recombination problem may be adapted from a similar problem that has already been solved: molecular reactions involving two species which combine in pairs.[34,35] A cursory analysis for a diffusion process would suggest that the concentration of electrons and holes would decay in time as $t^{-d/2}$, and indeed if the distributions of the two types of carriers were highly correlated, then the concentration would follow this form with $d=3$ for three-dimensional diffusion. However, often the two carrier distributions are independent of each other, at least over short distances. Consider a subvolume of the depletion region which, due to the variance of the Poisson distribution, has an excess of electrons at $t=0$. The holes in this section will be annihilated at some later time, but the remaining excess electrons will have to diffuse out of this region before encountering any additional holes, which will require more time, slowing the annihilation process. This effect is seen on all time and length scales and results in a concentration that decays as $t^{-d/4}$ rather than $t^{-d/2}$. If the particle concentrations are dependent over distances longer than some dependence length l_d, then the concentration will decay as $t^{-d/2}$ for time $t>t_1=l_d^2/\Delta$.[36,37] When an electron-hole pair is created, the electron and hole are initially displaced by a finite length, so the concentrations of electrons and holes will be highly correlated over regions larger than that mean length.

Including the effects of drift yields still other exponents. Here the distance traveled by a carrier along the direction of drift increases from $\sim t^{1/2}$ (diffusion alone) to $\sim t^1$ (with drift). Since there are d dimensions, the total volume swept out increases as $t^{d/2}$ with diffusion alone; with drift there are $d-1$ dimensions varying as $t^{1/2}$ each, and one varying as t^1, for a total volume in-

creasing as $t^{(d+1)/2}$. Since the particle concentration decays as the inverse square root of the volume encountered, it varies as $t^{-(d+1)/4}$ for independent electron and hole distributions and as $t^{-(d+1)/2}$ for dependent distributions.[38]

Now consider the point process corresponding to the times of the electron-hole recombinations. The decay of the number of electrons and holes is due to these recombinations, so the rate of recombination is equal to the rate of decrease of the number of particles. In the presence of drift and diffusion, the rate of recombination is therefore given by

$$h(t) \sim \begin{cases} 0, & t < A \\ t^{-1-(d+1)/4}, & A < t < B \\ t^{-1-(d+1)/2}, & t > B \end{cases} \quad (71)$$

where we identify $A = x_0^2/\Delta$ and $B = x_c^2/\Delta$, x_0 being a minimum separation for created electron-hole pairs, x_c being the maximum separation corresponding to a correlation length, and Δ being a combined effective diffusion constant. The impulse response function may be closely approximated by the form in Eq. (2), where $\beta = 1 + (d+1)/4$.

If energetic particles impinge on the detector at discrete times corresponding to a one-dimensional Poisson point process, then the resulting recombination process will be well described by the FSNDP. Thus the FSNDP should prove important in understanding the statistics of carrier recombination within the depletion region of the semiconductor particle detector.

2. *Diffusion on fractals*

Finally we turn to diffusion on fractals and percolation structures. In this case, the power-law exponent is given by $\beta = d_s/2$, where d_s is the spectral dimension of the fractal set, defined by

$$d_s \equiv 2d_f/(2+d_d) , \quad (72)$$

where d_f is the standard (Hausdorff) fractal dimension and d_d is the exponent describing the power-law variation of the diffusion constant with distance.[39,40] For percolation clusters at threshold, the spectral dimension lies between 1 and 2, and approaches a limit of $\frac{4}{3}$ for an infinite-dimensional embedding space.[40]

VI. CONCLUSION

In this paper we defined a new stochastic process, the FSNDP, which has unique properties. We then derived some of the statistical properties of the FSNDP, including its moment generating function, count moments and distribution, Fano factor, interevent time density, coincidence rate, and power spectral density. We showed that many of these statistics, especially the Fano factor and coincidence rate, exhibit power-law behavior over a significant range of times, indicating that the FSNDP is indeed fractal. In particular, for $0 < \beta < 1$ the resulting power spectral density varies as $f^{-\alpha}$, where the exponent α is defined by $\alpha \equiv 2(1-\beta)$ and varies between 0 and 2. For the particular case $\alpha = 1$, the power spectral density is precisely $1/f$. Moreover, such power-law behavior is prevalent in experimental time sequences, and thus the FSNDP is expected to be useful in understanding them. Finally, we considered two applications for the FSNDP of current interest in physics.

ACKNOWLEDGMENTS

This work was supported by the Joint Services Electronics Program through the Columbia Radiation Laboratory.

APPENDIX A: EQUIVALENCE OF STOCHASTIC-RATE AND CASCADE FORMULATIONS FOR THE SNDP

The SNDP may be formulated as a cluster process of the Neyman-Scott type or as a Poisson process with a stochastically varying shot-noise rate. These two formulations are isomorphic. We consider the moment generating function for the number of counts arriving in a time interval of duration T for a cluster process and show that this formulation yields results that are mathematically equivalent to those obtained from the stochastic rate approach. We use the results for shot noise and the SNDP number statistics as defined in Secs. III and IV B, respectively.

Suppose that the events from a primary homogeneous Poisson point process $M(t)$ with constant rate μ occur at times $\{t_j\}$, indexed by j, where j ranges from $-\infty$ to $+\infty$. Each primary event yields a random number of secondary events occurring at random delay times after the primary event. Let the number of secondary events occurring within the specified counting time window $[0,T]$, due to the primary event j occurring at t_j, be denoted by the random function $A(t_j)$. Since the secondary events are the result of an (inhomogeneous) Poisson process, $A(t_j)$ is Poisson distributed with

$$\langle A(t_j)|t_j \rangle_A = h_T(-t_j) = \int_0^T h(t-t_j)dt \quad (A1)$$

and with the corresponding moment generating function

$$Q_{A(t_j)}(s)|t_j = \exp[(e^{-s}-1)\langle A(t_j)|t_j \rangle_A] . \quad (A2)$$

The angular brackets with a subscript $\langle \ \rangle_x$ represent expectation over the distribution of the subscripted variable or process x.

The number of events n occurring in the interval $[0,T]$ is the sum of all the secondary events indexed by their respective primary events

$$n = \sum_j A(t_j) . \quad (A3)$$

Similarly, the integrated rate at any time t may be expressed as a sum of the integrated impulse response functions

$$W(t) = \sum_j h_T(t-t_j) . \quad (A4)$$

The moment generating function for the number of counts n becomes

$$Q_n(s)\equiv\langle\exp(-sn)\rangle_n=\left\langle\exp\left[-s\sum_j A(t_j)\right]\right\rangle_n=\left\langle\prod_j\exp[-sA(t_j)]\right\rangle_n=\left\langle\prod_j\langle\exp[-sA(t_j)]|t_j\rangle_A\right\rangle_{\{t_j\}}$$

$$=\left\langle\prod_j Q_{A(t_j)}(s)\,\middle|\,t_j\right\rangle_{\{t_j\}}=\left\langle\prod_j\exp[(e^{-s}-1)\langle A(t_j)|t_j\rangle]\right\rangle_{\{t_j\}}=\left\langle\exp\left[(e^{-s}-1)\sum_j h_T(t)\right]\right\rangle_{\{t_j\}}$$

$$=\langle\exp[(e^{-s}-1)W]\rangle_W=Q_W(1-e^{-s})\ . \tag{A5}$$

Thus the number of counts occurring in an arbitrary interval of length T, calculated within the framework of a cascade point process, is the Poisson transform of the integrated rate W, thereby demonstrating the equivalence of the two approaches. This result may be extended to encompass the multifold statistics of the SNDP, showing that the two formulations of the SNDP are entirely equivalent.

APPENDIX B: INTEGRATED FRACTAL-SHOT-NOISE CLOSED-FORM MOMENT GENERATING FUNCTION FOR $\beta=2$

In the special case $\beta=2$, $A=0$, $B=\infty$, deterministic K_0, and nonzero and finite T, a closed-form expression exists for the integrated fractal-shot-noise moment generating function $Q_W(s)$. If $s=0$, then $Q_W(0)=1$ follows from the definition of the moment generating function. For $s>0$, we begin with the form in Eq. (8),

$$\ln[Q_W(s)]=\int_{-\mu T}^{0}\left[\exp\left[-sK_0\mu\int_0^{y+\mu T}x^{-2}dx\right]-1\right]dy+\int_0^{\infty}\left[\exp\left[-sK_0\mu\int_y^{y+\mu T}x^{-2}dx\right]-1\right]dy$$

$$=-\mu T-\int_0^{\infty}\left[1-\exp\left[\frac{-sK_0\mu}{y^2+\mu Ty}\right]\right]dy\ . \tag{B1}$$

After integrating by parts and performing the substitution

$$u\equiv 1+\frac{(\mu T)^2/2}{y^2+\mu Ty}\ , \tag{B2}$$

we obtain

$$\ln[Q_W(s)]=-\mu T-\frac{\mu T}{2}\frac{2sK_0}{T}\exp\left[\frac{2sK_0}{T}\right]\int_1^{\infty}\left[\left[\frac{x+1}{x-1}\right]^{1/2}-1\right]\exp\left[-\frac{2sK_0}{T}x\right]dx$$

$$=-\mu T+\frac{\mu T}{2}-\mu sK_0\exp\left[\frac{2sK_0}{T}\right]\int_1^{\infty}\frac{1}{(x^2-1)^{1/2}}\exp\left[-\frac{2sK_0}{T}x\right]dx$$

$$-\mu sK_0\exp\left[\frac{2sK_0}{T}\right]\int_1^{\infty}\frac{x}{(x^2-1)^{1/2}}\exp\left[-\frac{2sK_0}{T}x\right]dx$$

$$=-\frac{\mu T}{2}-\mu s\mathcal{K}_0\left[\exp\left[\frac{2sK_0}{T}\right]\right]\left[\mathcal{K}_0\left[\frac{2sK_0}{T}\right]+\mathcal{K}_1\left[\frac{2sK_0}{T}\right]\right]\ . \tag{B3}$$

APPENDIX C: SHOT-NOISE AMPLITUDE DISTRIBUTION FOR INFINITE-AREA TAIL

For impulse response functions such that

$$\int_c^{\infty}h(t)dt=\infty \tag{C1}$$

for all $c<\infty$, the shot-noise process $I(t)$ will be infinite with probability one. To show this, we consider the moment generating function $Q_I(s)$ (Ref. 22) of the shot-noise process $I(t)$,

$$Q_I(s)\equiv\langle e^{-sI}\rangle_I$$

$$=\exp\left[-\mu\int_0^{\infty}\{1-\exp[-sh(t)]\}dt\right]\ . \tag{C2}$$

If $s=0$, then $Q_I(0)=1$ follows directly from the definition. Otherwise, for $s>0$, pick c and d such that

$$0<d\le\max\{sh(t)|c\le t\le\infty\}<\infty\ . \tag{C3}$$

Then

$$\int_0^{\infty}\{1-\exp[-sh(t)]\}dt\ge\frac{1-e^{-d}}{d}\int_c^{\infty}sh(t)dt=+\infty \tag{C4}$$

and, therefore,

$$Q_I(s)=\exp(-\mu\infty)=\exp(-\infty)=0\ . \tag{C5}$$

Thus $Q_I(s)$ is given by

$$Q_I(s)=\begin{cases}1, & s=0\\ 0, & s\neq 0\ ,\end{cases} \tag{C6}$$

so that

$$\Pr\{I<x\}=0 \quad \text{for all } x<\infty \ . \tag{C7}$$

APPENDIX D: SHOT-NOISE AMPLITUDE DISTRIBUTION FOR NORMALIZED INFINITE-AREA TAIL

For impulse response functions such that

$$\int_c^\infty g(t)dt=\infty \tag{D1}$$

for all $c<\infty$, the normalized shot-noise process $I(t)$ will approach a constant value. To show this, we construct a set of shot-noise processes $I_B(t)$, depending explicitly on the value of B, with corresponding impulse response functions

$$h_B(t)\equiv\begin{cases} qg(t), & A<t<B \\ 0, & \text{otherwise} \ , \end{cases} \tag{D2}$$

where the normalizing constant q is defined by

$$\int_0^\infty h_B(t)dt=q\int_A^B g(u)du=a \ . \tag{D3}$$

Thus the area a of the impulse response functions $h_B(t)$ is constant, while the duration $B-A$ increases without bound as B increases. The limiting process is then defined as

$$I(t)\equiv\lim_{B\to\infty} I_B(t) \ . \tag{D4}$$

The moment generating functions $Q_{IB}(s)$ approach a simple form $Q_I(s)=\exp(-as)$ in the limit $B\to\infty$. We consider the negative logarithm of the moment generating function of the representative shot-noise process $I_B(t)$ and first find an upper bound:

$$\begin{aligned} -\ln[Q_{IB}(s)]&=\int_A^B\{1-\exp[sqg(t)]\}dt \\ &\le\int_A^B sqg(t)dt=as \ . \end{aligned} \tag{D5}$$

For a lower bound we truncate the integral at some value c,

$$\begin{aligned} -\ln[Q_{IB}(s)]&=\int_A^B\{1-\exp[sqg(t)]\}dt\ge\int_c^B\{1-\exp[sqg(t)]\}dt \\ &\ge\frac{1-\exp[sqg(c)]}{sqg(c)}\int_c^B sqg(t)dt=\frac{1-\exp[sqg(c)]}{sqg(c)}\frac{\int_c^B g(t)dt}{\int_A^B g(t)dt}as \\ &\to\frac{1-\exp[sqg(c)]}{sqg(c)}as \ , \end{aligned} \tag{D6}$$

as $B\to\infty$. Thus for the limiting process, we have

$$as\frac{1-\exp[sqg(c)]}{sqg(c)}\le-\ln[Q_I(s)]\le as \ . \tag{D7}$$

Since we can pick c to be any large number, the fraction in Eq. (D7) can be made as close to unity as desired, resulting in

$$as\le-\ln[Q_I(s)]\le as \ , \tag{D8}$$

which leads to

$$Q_I(s)=\exp(-as) \ , \tag{D9}$$

proving that the normalized shot-noise processes $I_B(t)$ tend in distribution to a constant value equal to the area a of the impulse response function as B increases towards infinity.

APPENDIX E: INTEGRALS FOR FRACTAL SNDP TIME AND NUMBER STATISTICS

Because the time and number statistics of the SNDP can become quite complex when the power-law form $Kt^{-\beta}$ is substituted for $h(t)$, the details are provided in this appendix rather than in the body of the paper. The pertinent figures were generated by numerically integrating the resultant expressions.

For the time statistics we begin with $p(0)$ and obtain its first two derivatives. We consider the case for deterministic K_0. From Eqs. (18) and (53) we have

$$\Pr\{n=0\}=p(0)=Q_W(1)=P_0(t)=\exp\left[\mu\int_{-\infty}^\infty\{\exp[-h_T(t)]-1\}du\right]=\exp[\mu f(T)] \ , \tag{E1}$$

where $f(T)$, implicitly defined in Eq. (E1), is employed to simplify notation. The forward recurrence time probability density is given by

$$P_1(\tau)=-\frac{d}{dT}P_0(T)\bigg|_{T=\tau}=-\mu P_0(\tau)\frac{df(\tau)}{d\tau}\ , \tag{E2}$$

whereas the interevent time density is given by

$$P_2(\tau)=-\frac{1}{\langle I\rangle_I}\frac{d^2}{dT^2}P_0(T)\bigg|_{T=\tau}=\frac{\mu}{a}P_0(\tau)\left[\left[\frac{df(\tau)}{d\tau}\right]^2+\frac{d^2f(\tau)}{d\tau^2}\right]\ . \tag{E3}$$

Thus $P_0(\tau)$, $P_1(\tau)$, and $P_2(\tau)$ depend in turn on $f(\tau)$ and its first two derivatives, which are provided below.

The function $f(\tau)$ assumes four different forms, depending on the value of β and the relative magnitudes of A, B, and τ.

For $\beta\neq 1$ and $B>A+\tau$,

$$\begin{aligned}
f(\tau)&=\int_A^{A+\tau}\left[\exp\left[-\frac{K_0}{1-\beta}(u^{1-\beta}-A^{1-\beta})\right]-1\right]du+\int_A^{B-\tau}\left[\exp\left[-\frac{K_0}{1-\beta}[(u+\tau)^{1-\beta}-u^{1-\beta}]\right]-1\right]du\\
&\quad+\int_{B-\tau}^{B}\left[\exp\left[-\frac{K_0}{1-\beta}(B^{1-\beta}-u^{1-\beta})\right]-1\right]du\ ,\\
-\frac{df(\tau)}{d\tau}&=K_0\int_A^{B-\tau}(u+\tau)^{-\beta}\exp\left[-\frac{K_0}{1-\beta}[(u+\tau)^{1-\beta}-u^{1-\beta}]\right]du+\left[1-\exp\left[-\frac{K_0}{1-\beta}[(A+\tau)^{1-\beta}-A^{1-\beta}]\right]\right]\ ,\\
\frac{d^2f(\tau)}{d\tau^2}&=K_0B^{-\beta}\exp\left[-\frac{K_0}{1-\beta}[B^{1-\beta}-(B-\tau)^{1-\beta}]\right]-K_0(A+\tau)^{-\beta}\exp\left[-\frac{K_0}{1-\beta}[(A+\tau)^{1-\beta}-A^{1-\beta}]\right]\\
&\quad+K_0\int_{A+\tau}^{B}(\beta u^{-\beta-1}+K_0u^{-2\beta})\exp\left[-\frac{K_0}{1-\beta}[u^{1-\beta}-(u-\tau)^{1-\beta}]\right]du\ .
\end{aligned} \tag{E4}$$

For $\beta\neq 1$ and $B\leq A+\tau$,

$$\begin{aligned}
f(\tau)&=\int_A^{B}\left[\exp\left[-\frac{K_0}{1-\beta}(u^{1-\beta}-A^{1-\beta})\right]-1\right]du+(\tau+A-B)(e^{-a}-1)\\
&\quad+\int_A^{B}\left[\exp\left[-\frac{K_0}{1-\beta}(B^{1-\beta}-u^{1-\beta})\right]-1\right]du\ ,\\
-\frac{df(\tau)}{d\tau}&=1-e^{-a}\ ,\\
\frac{d^2f(\tau)}{d\tau^2}&=0\ .
\end{aligned} \tag{E5}$$

For $\beta=1$ and $B>A+\tau$,

$$\begin{aligned}
f(\tau)&=\int_A^{B-\tau}\left[\left[\frac{u}{u+\tau}\right]^{K_0}-1\right]du+\int_A^{A+\tau}\left[\left[\frac{A}{u}\right]^{K_0}-1\right]du+\int_{B-\tau}^{B}\left[\left[\frac{u}{B}\right]^{K_0}-1\right]du\ ,\\
-\frac{df(\tau)}{d\tau}&=K_0\int_A^{B-\tau}\frac{u^{K_0}}{(u+\tau)^{K_0+1}}du-\left[\left[\frac{A}{A+\tau}\right]^{K_0}-1\right]\ ,\\
\frac{d^2f(\tau)}{d\tau^2}&=K_0\frac{(B-\tau)^{K_0}}{B^{K_0+1}}-K_0\frac{A^{K_0}}{(A+\tau)^{K_0+1}}-K_0(K_0+1)\int_A^{B-\tau}\frac{u^{K_0}}{(u+\tau)^{K_0+2}}du\ .
\end{aligned} \tag{E6}$$

For $\beta=1$ and $B\leq A+\tau$,

$$\begin{aligned}
f(\tau)&=\int_A^{B}\left[\left[\frac{A}{u}\right]^{K_0}-1\right]du+\int_A^{B}\left[\left[\frac{u}{B}\right]^{K_0}-1\right]du+(\tau+A-B)\left[\left[\frac{A}{B}\right]^{K_0}-1\right]\ ,\\
-\frac{df(\tau)}{d\tau}&=1-\left[\frac{A}{B}\right]^{K_0}\ ,\\
\frac{d^2f(\tau)}{d\tau^2}&=0\ .
\end{aligned} \tag{E7}$$

The counting distribution of the FSNDP is determined by a recursion relation. We again consider the case for deterministic K_0. From Eqs. (16) and (17) we have

$$p(m+1)=\frac{1}{m+1}\sum_{i=0}^{m} c_i p(m-i) \tag{E8}$$

and

$$c_i \equiv \frac{\mu}{i!}\left\langle \int_{-\infty}^{\infty} [h_T(K,t)]^{i+1}\exp[-h_T(K,t)]dt \right\rangle . \tag{E9}$$

The recursion coefficients c_i have four different forms, depending on the value of β and the relative magnitudes of A, B, and T.

For $\beta \neq 1$ and $B > A+T$,

$$\begin{aligned} c_i=\frac{\mu K_0^{i+1}}{i!(1-\beta)^{i+1}} \Bigg[& \int_A^{A+T} (u^{1-\beta}-A^{1-\beta})^{i+1}\exp\left[-\frac{K_0}{1-\beta}(u^{1-\beta}-A^{1-\beta})\right]du \\ & + \int_A^{B-T} [(u+T)^{1-\beta}-u^{1-\beta}]^{i+1}\exp\left[-\frac{K_0}{1-\beta}[(u+T)^{1-\beta}-u^{1-\beta}]\right]du \\ & + \int_{B-T}^{B} (B^{1-\beta}-u^{1-\beta})^{i+1}\exp\left[-\frac{K_0}{1-\beta}(B^{1-\beta}-u^{1-\beta})\right]du \Bigg] . \end{aligned} \tag{E10}$$

For $\beta \neq 1$ and $B \leq A+T$,

$$\begin{aligned} c_i=\frac{\mu K_0^{i+1}}{i!(1-\beta)^{i+1}} \Bigg[& \int_A^{B} (u^{1-\beta}-A^{1-\beta})^{i+1}\exp\left[-\frac{K_0}{1-\beta}[(u+T)^{1-\beta}-A^{1-\beta}]\right]du \\ & + \int_A^{B} (B^{1-\beta}-u^{1-\beta})^{i+1}\exp\left[-\frac{K_0}{1-\beta}(B^{1-\beta}-u^{1-\beta})\right]du \\ & + (T+A-B)(B^{1-\beta}-A^{1-\beta})^{i+1}\exp\left[-\frac{K_0}{1-\beta}(B^{1-\beta}-A^{1-\beta})\right] \Bigg] . \end{aligned} \tag{E11}$$

For $\beta = 1$ and $B > A+T$,

$$\begin{aligned} c_i=\frac{\mu K_0^{i+1}}{i!} \Bigg\{ & \int_A^{B-T} \left[\ln\left[\frac{u+T}{u}\right]\right]^{i+1}\left[\frac{u}{u+T}\right]^{K_0}du \\ & + \int_A^{A+T} \left[\ln\left[\frac{u}{A}\right]\right]^{i+1}\left[\frac{A}{u}\right]^{K_0}du + \int_{B-T}^{B} \left[\ln\left[\frac{B}{u}\right]\right]^{i+1}\left[\frac{u}{B}\right]^{K_0}du \Bigg\} . \end{aligned} \tag{E12}$$

For $\beta = 1$ and $B \leq A+T$,

$$c_i=\frac{\mu K_0^{i+1}}{i!}\left\{(T+A-B)\left[\ln\left[\frac{B}{A}\right]\right]^{i+1}\left[\frac{A}{B}\right]^{K_0} + \int_A^{B}\left[\ln\left[\frac{u}{A}\right]\right]^{i+1}\left[\frac{A}{u}\right]^{K_0}du + \int_A^{B}\left[\ln\left[\frac{B}{u}\right]\right]^{i+1}\left[\frac{u}{B}\right]^{K_0}du\right\} . \tag{E13}$$

The count moments of the FSNDP are also determined by a recursion relation, but in this case we can easily consider stochastic K in addition to deterministic K_0. From Eqs. (23) and (24) we have

$$F_n^{(m+1)}=\sum_{i=0}^{m} b_i \begin{bmatrix} m \\ i \end{bmatrix} F_n^{(m-i)}, \quad F_n^{(0)} \equiv 1 \tag{E14}$$

and

$$b_i \equiv \mu\left\langle \int_{-\infty}^{\infty} [h_T(K,t)]^{i+1}dt \right\rangle . \tag{E15}$$

The recursion coefficients b_i have four different forms, depending on β and the relative magnitudes of A, B, and T.

For $\beta \neq 1$ and $B > A+T$,

$$\begin{aligned} b_i=\frac{\mu\langle K^{i+1}\rangle}{i!(1-\beta)^{i+1}} \Bigg[& \int_A^{B-T} [(u+T)^{1-\beta}-u^{1-\beta}]^{i+1}du \\ & + \int_A^{A+T} (u^{1-\beta}-A^{1-\beta})^{i+1}du \\ & + \int_{B-T}^{B} (B^{1-\beta}-u^{1-\beta})^{i+1}du \Bigg] . \end{aligned} \tag{E16}$$

For $\beta \neq 1$ and $B \leq A+T$,

$$b_i = \frac{\mu\langle K^{i+1}\rangle}{i!(1-\beta)^{i+1}} \left[(T+A-B)(B^{1-\beta}-A^{1-\beta})^{i+1} + \int_A^B (u^{1-\beta}-A^{1-\beta})^{i+1} du + \int_A^B (B^{1-\beta}-u^{1-\beta})^{i+1} du \right] . \quad \text{(E17)}$$

For $\beta = 1$ and $B > A+T$,

$$b_i = \frac{\mu\langle K^{i+1}\rangle}{i!} \left\{ \int_A^{B-T} \left[\ln\left[\frac{u+T}{u} \right] \right]^{i+1} du + \int_A^{A+T} \left[\ln\left[\frac{u}{A} \right] \right]^{i+1} du + \int_{B-T}^{B} \left[\ln\left[\frac{B}{u} \right] \right]^{i+1} du \right\} . \quad \text{(E18)}$$

For $\beta = 1$ and $B \leq A+T$,

$$b_i = \frac{\mu\langle K^{i+1}\rangle}{i!} \left\{ (T+A-B) \left[\ln\left[\frac{B}{A} \right] \right]^{i+1} + \int_A^B \left[\ln\left[\frac{u}{A} \right] \right]^{i+1} du + \int_A^B \left[\ln\left[\frac{B}{u} \right] \right]^{i+1} du \right\} . \quad \text{(E19)}$$

APPENDIX F: EXACT AND LIMITING FORMS FOR THE FANO FACTOR

Closed-form expressions for the FSNDP Fano factor do not exist in general, although such forms may be obtained in some special cases and limits. We present below a more detailed treatment of these expressions than in the body of the paper.

For $\beta = \frac{1}{2}$ the Fano factor becomes

$$F = 1 + \frac{\langle K^2\rangle}{T\langle K\rangle(B^{1/2}-A^{1/2})} \times \int_0^L (T-u) \int_A^{B-u} (t^2+ut)^{-1/2} dt\, du , \quad \text{(F1)}$$

where the upper limit of the outer integral is defined as

$$L \equiv \min(T, B-A) . \quad \text{(F2)}$$

For the inner integral we have

$$\int_A^{B-u} (t^2+ut)^{-1/2} dt = 2\{\ln[t^{1/2}+(t+u)^{1/2}]\}_A^{B-u} , \quad \text{(F3)}$$

so that the outer integral simplifies to

$$2\int_0^L (T-u)\ln[1+(1-u/B)^{1/2}]du - 2\int_0^L (T-u)\ln[1+(1+u/A)^{1/2}]du + \ln\left[\frac{B^{1/2}}{A^{1/2}} \right](2TL-L^2) . \quad \text{(F4)}$$

The remaining integrals are of the form

$$2\int_0^L (T-u)\ln[1+(1+u/c)^{1/2}]du . \quad \text{(F5)}$$

We make the substitution $v \equiv (1+u/c)^{1/2}$, whereupon the integral in Eq. (F5) becomes

$$4c(T+c)\int_1^{(1+L/c)^{1/2}} v\ln(1+v)dv - 4c^2\int_1^{(1+L/c)^{1/2}} v^3\ln(1+v)dv = L(2T-L)\ln[1+(1+L/c)^{1/2}] + c(\tfrac{2}{3}c+2T-\tfrac{1}{3}L)(1+L/c)^{1/2} - \tfrac{2}{3}c^2 - 2cT - TL + \tfrac{1}{4}L^2 . \quad \text{(F6)}$$

This yields the following for the Fano factor itself:

$$F = 1 + \frac{\langle K^2\rangle}{T\langle K\rangle(B^{1/2}-A^{1/2})} \left[L(2T-L)\ln\left[\frac{B^{1/2}+(B-L)^{1/2}}{A^{1/2}+(A+L)^{1/2}} \right] + \tfrac{1}{3}(L-6T+2B)(B^2-BL)^{1/2} + \tfrac{1}{3}(L-6T-2A)(A^2+AL)^{1/2} - \tfrac{2}{3}(B^2-A^2) + 2T(B+A) \right] . \quad \text{(F7)}$$

Finally, we substitute the smaller of $B-A$ and T for L to obtain Eqs. (31) and (32).

For $\beta = 2$ the Fano factor becomes

$$F = 1 + \frac{2AB\langle K^2\rangle}{T(B-A)\langle K\rangle} \int_0^L (T-u) \int_A^{B-u} (t^2+ut)^{-2} dt\, du , \quad \text{(F8)}$$

with L defined as above. For the inner integral we have

$$\int_A^{B-u} (t^2+ut)^{-2} dt\, du = \int_A^{B-u} \frac{1}{u^3} \left[\frac{u}{t^2} + \frac{u}{(t+u)^2} - \frac{2}{t} + \frac{2}{t+u} \right] dt = u^{-3} \left[-\frac{u}{t} - \frac{u}{t+u} - 2\ln(t) + 2\ln(t+u) \right]_A^{B-u} , \quad \text{(F9)}$$

so that the outer integral simplifies to

$$\left[\frac{T}{u^2}-\frac{2}{u}-\frac{1}{A}\right]\ln(1+u/A)-\frac{T}{Au}+\left[\frac{T}{u^2}-\frac{2}{u}+\frac{1}{B}\right]\ln(1-u/B)+\frac{T}{Bu}\Bigg|_0^L . \tag{F10}$$

The integral is not defined in the limit $u\to 0$, so we must use l'Hôpital's rule:

$$\lim_{u\to 0}\left[\left[\frac{T}{u^2}-\frac{2}{u}-\frac{1}{A}\right]\ln(1+u/A)-\frac{T}{Au}\right]=T\lim_{u\to 0}\frac{\ln(1+u/A)-u/A}{u^2}-2\lim_{u\to 0}\frac{\ln(1+u/A)}{u}-\frac{1}{A}\lim_{u\to 0}\ln(1+u/A)$$
$$=-\frac{T}{2A^2}-\frac{2}{A}-0 . \tag{F11}$$

Similarly, for B we obtain $-T/2B^2+2/B$. This yields the following for the Fano factor itself:

$$F=1+\frac{2AB\langle K^2\rangle}{T(B-A)\langle K\rangle}\left[\frac{T}{2A^2}+\frac{2}{A}-\frac{T}{AL}+\frac{T}{2B^2}-\frac{2}{B}+\frac{T}{BL}+\left[\frac{T}{L^2}-\frac{2}{L}-\frac{1}{A}\right]\ln(1+L/A)\right.$$
$$\left.+\left[\frac{T}{L^2}-\frac{2}{L}+\frac{1}{B}\right]\ln(1-L/B)\right] . \tag{F12}$$

Finally, we substitute the smaller of $B-A$ and T for L to obtain Eqs. (33) and (34).

Approximate expressions for the Fano factor may be found for arbitrary β in the following limits: $T\ll A$, $A\ll T\ll B$, and $T\gg B$. Rather than considering limits of the entire Fano factor expression

$$F=1+\frac{2\langle K^2\rangle}{T\langle K\rangle\int_A^B t^{-\beta}dt}\times\int_0^L(T-u)\int_A^{B-u}(t^2+ut)^{-\beta}dt\,du , \tag{F13}$$

we obtain limits for the integrals within the expression.

For $T\ll A$, $L=T$. By using l'Hôpital's rule twice, we obtain

$$\lim_{T\to 0}\int_0^T(T-u)\int_A^{B-u}(t^2+ut)^{-\beta}dt\,du/T^2=\tfrac{1}{2}\int_A^B(t^2)^{-\beta}dt , \tag{F14}$$

so that for small T,

$$F\approx 1+\frac{\langle K^2\rangle\int_A^B t^{-2\beta}dt}{\langle K\rangle\int_A^B t^{-\beta}dt}T . \tag{F15}$$

For $A\ll T\ll B$, again we have $L=T$, but now the limiting expression depends on β. Since in this case $A\ll B$, the integral in the denominator of the Fano factor expression will tend to a simple limit,

$$\int_A^B t^{-\beta}dt\to\begin{cases}B^{1-\beta}/(1-\beta), & \beta<1\\ \ln(B/A), & \beta=1 ,\\ A^{1-\beta}/(\beta-1), & \beta>1 .\end{cases} \qquad B/A\to\infty \tag{F16}$$

The double integral in the numerator of Eq. (F13), henceforth denoted $\int\int$, is more complicated; we consider in turn five expressions for different ranges of β. For $0<\beta<\frac{1}{2}$, we define $x\equiv A/T$ and $y\equiv B/T$. Then

$$\int\int=T^{3-2\beta}\int_0^1(1-u)\int_x^{y-u}(t^2+ut)^{-\beta}dt\,du . \tag{F17}$$

We fix $x=0$ and use l'Hôpital's rule to obtain

$$\lim_{y\to\infty}\int_0^1(1-u)\int_0^{y-u}(t^2+ut)^{-\beta}dt\,du/y^{1-2\beta}=[2(1-2\beta)]^{-1} . \tag{F18}$$

So the Fano factor is given by

$$F\approx 1+\frac{\langle K^2\rangle(1-\beta)}{\langle K\rangle(1-2\beta)}B^{-\beta}T . \tag{F19}$$

If $\beta=\frac{1}{2}$, we again fix $x=0$ and obtain with l'Hôpital's rule,

$$\lim_{y\to\infty}\int_0^1(1-u)\int_0^{y-u}(t^2+ut)^{-1/2}dt\,du/\ln(y)=\tfrac{1}{2} , \tag{F20}$$

so that

$$F\approx 1+\frac{\langle K^2\rangle}{2\langle K\rangle}B^{-1/2}[\ln(B/T)]T . \tag{F21}$$

For $\frac{1}{2}<\beta<1$, we consider the limits where both $x\to 0$ and $y\to\infty$. Here the integral in the numerator becomes

$$\int\int=T^{3-2\beta}\int_0^1(1-u)\int_0^{\infty}(t^2+ut)^{-\beta}dt\,du$$
$$=T^{3-2\beta}\frac{1}{2(1-\beta)(3-2\beta)}\frac{\Gamma(1-\beta)\Gamma(2\beta-1)}{\Gamma(\beta)} , \tag{F22}$$

so that the Fano factor is given by

$$F\approx 1+\frac{\langle K^2\rangle\Gamma(1-\beta)\Gamma(2\beta-1)}{\langle K\rangle(3-2\beta)\Gamma(\beta)}B^{\beta-1}T^{2(1-\beta)} . \tag{F23}$$

For $\beta=1$ we define $x\equiv T/A$ and $y\equiv T/B$. Then

$$\int\int = \int_0^T (T-u)\int_A^{B-u}(t^2+ut)^{-1}dt\,du$$
$$= T\int_0^1 \frac{1-u}{u}\ln(1-yu)du + T\int_0^1 \frac{1-u}{u}\ln(1+xu)du . \tag{F24}$$

The first term approaches zero as $y\to 0$ since

$$0 > \int_0^1 \frac{1-u}{u}\ln(1-yu)du > \int_0^1 \frac{1-u}{u}u\ln(1-y)du$$
$$= (T/2)\ln(1-y) \tag{F25}$$

and $\ln(1-y)\to 0$ as $y\to 0$. For the second term, two applications of l'Hôpital's rule and some simplification yield

$$\lim_{x\to\infty}\int_0^1 \frac{1-u}{u}\ln(1+xu)du \Big/ \ln^2(x) = 1 . \tag{F26}$$

The Fano factor is therefore given by

$$F \approx 1+\frac{2\langle K^2\rangle}{\langle K\rangle}\frac{\ln^2(T/A)}{\ln(B/A)} . \tag{F27}$$

Finally, for $\beta > 1$ we define $x \equiv T/A$ and $y \equiv B/T$, and

$$\int\int = A^{3-2\beta}\int_0^x (x-u)\int_1^{xy-u}(t^2+ut)^{-\beta}dt\,du . \tag{F28}$$

We fix $y > 1$ and use l'Hôpital's rule to obtain

$$\lim_{x\to\infty}\int_0^x (x-u)\int_1^{xy-u}(t^2+ut)^{-\beta}dt\,du \Big/ x$$
$$= [2(\beta-1)^2]^{-1} . \tag{F29}$$

The Fano factor is thus given by

$$F \approx 1+\frac{\langle K^2\rangle}{\langle K\rangle(\beta-1)}A^{1-\beta} . \tag{F30}$$

For $T \gg B$, $L = B - A$. Using the substitution $v \equiv t+u$ and interchanging the order of integration in the numerator yields

$$F = 1+\frac{2\langle K^2\rangle}{\langle K\rangle}\int_A^B t^{-\beta} \times \int_t^B [1+(t-v)/T]v^{-\beta}dv\,dt \Big/ \int_A^B t^{-\beta}dt . \tag{F31}$$

In the limit $T \gg B$, the $(t-v)$ term in the numerator vanishes so that

$$F \approx 1+\frac{2\langle K^2\rangle}{\langle K\rangle}\int_A^B t^{-\beta}\int_t^B v^{-\beta}dv\,dt \Big/ \int_A^B t^{-\beta}dt$$
$$= 1+\frac{2\langle K^2\rangle}{\langle K\rangle}\frac{1}{2}\left[\int_A^B t^{-\beta}dt\right]^{-2} \Big/ \int_A^B t^{-\beta}dt$$
$$= 1+\frac{\langle K^2\rangle}{\langle K\rangle}\int_A^B t^{-\beta}dt . \tag{F32}$$

APPENDIX G: NORMALIZED COINCIDENCE RATE

The normalized coincidence rate is a measure of the correlation between events with a specified time delay between them and is defined as

$$g^{(2)}(\tau) \equiv \lim_{\Delta T\to 0}\frac{\Pr\{\mathcal{E}(\tau,\tau+\Delta T)\text{ and }\mathcal{E}(0,\Delta T)\}}{\Pr\{\mathcal{E}(\tau,\tau+\Delta T)\}\Pr\{\mathcal{E}(0,\Delta T)\}} . \tag{G1}$$

For a SNDP, we use stationarity and the definition of a Poisson process to obtain

$$\Pr\{\mathcal{E}(\tau,\tau+\Delta T)\} = \Pr\{\mathcal{E}(0,\Delta T)\} = \langle I\rangle_I \Delta T = \mu a\Delta T . \tag{G2}$$

For the joint event we condition on the value of the driving shot-noise process $I(t)$, yielding

$$\Pr\{\mathcal{E}(\tau,\tau+\Delta T)\text{ and }\mathcal{E}(0,\Delta T)\}$$
$$= \int_x\int_y \Pr\{\mathcal{E}(\tau,\tau+\Delta T)\text{ and }\mathcal{E}(0,\Delta T)|I(0)=x\text{ and }I(\tau)=y\}\Pr\{I(0)\in dx\text{ and }I(\tau)\in dy\}$$
$$= \int_x\int_y I(0)(\Delta T)I(\tau)(\Delta T)\Pr\{I(0)\in dx\text{ and }I(\tau)\in dy\} = (\Delta T)^2\langle I(0)I(\tau)\rangle_I$$
$$= \mu^2a^2(\Delta T)^2 + \mu(\Delta T)^2\left\langle\int_{-\infty}^{\infty}h(K,t)h(K,t+\tau)\right\rangle dt . \tag{G3}$$

Therefore, the coincidence rate is given by

$$g^{(2)}(\tau) = \lim_{\Delta T\to 0}\mu^2a^2\left[(\Delta T)^2+\mu(\Delta T)^2\left\langle\int_{-\infty}^{\infty}h(K,t)h(K,t+\tau)dt\right\rangle\right]\Big/\mu^2a^2(\Delta T)^2$$
$$= 1+\frac{1}{\mu a^2}\left\langle\int_{-\infty}^{\infty}h(K,t)h(K,t+\tau)\right\rangle dt . \tag{G4}$$

In the limits $\tau \ll A$ and $A \ll \tau \ll B$, the coincidence rate approaches a simpler form which may be found by arguments similar to those used for the Fano factor, except for the case $A \ll \tau \ll B$ and $\beta > 1$, where unbounded area near the onset of the impulse response function makes the resulting point process intractable. In that case we use l'Hôpital's rule to obtain

$$\lim_{A\to 0}\int_A^{B-\tau}(t^2+\tau t)^{-\beta}dt \Big/ \int_A^B t^{-\beta}dt = \tau^{-\beta} . \tag{G5}$$

Therefore, for $\beta > 1$ and in the limit $A \ll \tau \ll B$, we have

$$g^{(2)}(\tau) \to 1+(\langle K^2\rangle/\mu\langle K\rangle^2)(\beta-1)A^{\beta-1}\tau^{-\beta} . \tag{G6}$$

[1]F. A. Haight, *Handbook of the Poisson Distribution* (Wiley, New York, 1967).
[2]D. R. Cox, J. R. Stat. Soc., Ser. B **17**, 129 (1955).
[3]E. M. Purcell, Nature **178**, 1449 (1956).
[4]W. J. McGill, J. Math. Psychol. **4**, 351 (1967).
[5]M. C. Teich, P. R. Prucnal, G. Vannucci, M. E. Breton, and W. J. McGill, J. Opt. Soc. Am. **72**, 419 (1982).
[6]B. E. A. Saleh and M. C. Teich, Proc. IEEE **70**, 229 (1982).
[7]A. J. Lawrance, in *Stochastic Point Processes: Statistical Analysis, Theory, and Applications,* edited by P. A. W. Lewis (Wiley-Interscience, New York, 1972), p. 199.
[8]M. S. Bartlett, Biometrika **51**, 299 (1964).
[9]M. C. Teich, R. G. Turcott, and S. B. Lowen, in *Mechanics and Biophysics of Hearing,* edited by P. Dallos, C. D. Geisler, J. W. Matthews, M. A. Ruggiero, and C. R. Steele (Springer, New York, 1990).
[10]M. S. Bartlett, J. R. Stat. Soc., Ser. B **25**, 264 (1963).
[11]P. A. W. Lewis, J. R. Stat. Soc., Ser. B **26**, 398 (1964).
[12]J. Neyman and E. L. Scott, J. R. Stat. Soc., Ser. B **20**, 1 (1958).
[13]J. Neyman and E. L. Scott, in *Stochastic Point Processes: Statistical Analysis, Theory, and Applications,* edited by P. A. W. Lewis (Wiley-Interscience, New York, 1972), p. 646.
[14]K. Matsuo, B. E. A. Saleh, and M. C. Teich, J. Math. Phys. **23**, 2353 (1982).
[15]K. Matsuo, M. C. Teich, and B. E. A. Saleh, J. Math. Phys. **25**, 2174 (1984).
[16]S. B. Lowen and M. C. Teich, Electron. Lett. **25**, 1072 (1989).
[17]S. B. Lowen and M. C. Teich, Phys. Rev. Lett. **63**, 1755 (1989).
[18]S. B. Lowen and M. C. Teich, IEEE Trans. Inf. Theory **36**, 1302 (1990).
[19]N. Campbell, Proc. Cambridge Philos. Soc. **15**, 117 (1909).
[20]N. Campbell, Proc. Cambridge Philos. Soc. **15**, 310 (1909).
[21]W. Feller, *An Introduction to Probability Theory and its Applications,* 3rd ed. (Wiley, New York, 1971), Vol. 2.
[22]J. L. Doob, *Stochastic Processes* (Wiley, New York, 1953).
[23]B. E. A. Saleh, *Photoelectron Statistics* (Springer-Verlag, Berlin, 1978).
[24]M. C. Teich and B. E. A. Saleh, Phys. Rev. A **24**, 1651 (1981).
[25]J. Neyman, Ann. Math. Stat. **10**, 35 (1939).
[26]M. C. Teich and B. E. A. Saleh, J. Mod. Opt. **34**, 1169 (1987).
[27]W. Feller, Ann. Math. Stat. **14**, 389 (1943).
[28]U. Fano, Phys. Rev. **72**, 26 (1947).
[29]D. R. Cox and P. A. W. Lewis, *The Statistical Analysis of Series of Events* (Methuen, London, 1966).
[30]J. V. Jelley, *Čerenkov Radiation* (Pergamon, London, 1958).
[31]V. P. Zrelov, *Cherenkov Radiation in High-Energy Physics, Part I* (Atomizdat, Moscow, 1968) (Translation: Israel Program for Scientific Translations, Jerusalem, 1970).
[32]M. A. Pinsky, *Introduction to Partial Differential Equations with Applications* (McGraw-Hill, New York, 1984).
[33]G. F. Knoll, *Radiation Detection and Measurement,* 2nd ed. (Wiley, New York, 1989).
[34]S. F. Burlatsky, G. S. Oshanin, and A. A. Ovchinnikov, Phys. Lett. **139A**, 241 (1989).
[35]G. S. Oshanin, S. F. Burlatsky, and A. A. Ovchinnikov, Phys. Lett. **139A**, 245 (1989).
[36]A. A. Ovchinnikov and Y. B. Zeldovich, Chem. Phys. **28**, 215 (1978).
[37]D. Toussaint and F. Wilczek, J. Chem. Phys. **78**, 2642 (1983).
[38]K. Kang and S. Redner, Phys. Rev. Lett. **52**, 955 (1984).
[39]S. Alexander and R. Orbach, J. Phys. (Paris) Lett. **43**, L625 (1982).
[40]R. Rammal and G. Toulouse, J. Phys. (Paris) Lett. **44**, L13 (1983).